2011

Hydraulics, Morphology, and Energy Dissipation in an Alpine Step-pool Channel

Andrew C. Wilcox
University of Montana - Missoula, andrew.wilcox@umontana.edu

Ellen E. Wohl

Francesco Comiti

Luca Mao

Hydraulics, morphology, and energy dissipation in an alpine step-pool channel

Andrew C. Wilcox,[1] Ellen E. Wohl,[2] Francesco Comiti,[3] and Luca Mao[4]

Received 29 October 2010; revised 22 March 2011; accepted 4 April 2011; published 8 July 2011.

[1] To investigate the relationship between hydraulics and channel morphology in step-pool channels, we combined three-dimensional velocity measurements with an acoustic Doppler velocimeter and topographic surveys in a steep step-pool channel, the Rio Cordon, Italy. Measurements were organized around step, pool, and tread units and occurred within a range of 36%–57% of bankfull discharges. As flow moved from steps to their downstream pools in our study reach, an average of approximately two thirds of the total energy was dissipated, as measured by relative head loss through step-pool sequences. Much of this head loss was achieved by elevation (potential energy) loss rather than velocity reductions. Although an overall, expected pattern of flow acceleration toward step crests and deceleration in pools was present, pool velocities were high, especially where upstream step crests were irregular and where residual pool depths were low. Many steps were porous or "leaky," with irregular cross-channel bed and water surface topography, producing high-velocity jets and less flow resistance than channel-spanning dammed steps. Longitudinal variations in hydraulics are thus often overshadowed by lateral variations arising from morphologic complexities. Velocity and turbulence characteristics in the Rio Cordon show marked differences from data we have collected in a more stable and wood-rich channel in the Colorado Rockies, in which "ponded" steps are more prevalent and pools are slower and more turbulent. Comparison of these channels illustrates that step-pool structure and hydraulics are strongly influenced by flow regime, sediment supply, lithology, time since the last step-forming flood, and availability of in-stream wood.

Citation: Wilcox, A. C., E. E. Wohl, F. Comiti, and L. Mao (2011), Hydraulics, morphology, and energy dissipation in an alpine step-pool channel, *Water Resour. Res.*, *47*, W07514, doi:10.1029/2010WR010192.

1. Introduction

[2] Step-pool sequences, in which flow plunges over channel-spanning boulder, log, and/or bedrock steps into downstream scour pools, produce stepped longitudinal profiles and dissipate energy in high-gradient streams [*Keller and Swanson*, 1979; *Montgomery and Buffington*, 1997; *Chin and Wohl*, 2005; *Church and Zimmermann*, 2007]. Further understanding of feedbacks between hydraulics and bed morphology is critical to developing insight into sediment transport and formative processes in these channels. Step-pool channels are important because of their position in the headwaters of many drainage networks, where they constitute a large proportion of channel length, provide habitat for a variety of aquatic species, and influence the fluxes of water, sediment and nutrients to downstream areas [*Wohl*, 2000; *Benda et al.*, 2005; *Freeman et al.*, 2007]. Analogies between step-pool sequences and engineered structures for energy dissipation have also motivated investigations of steep channels, especially where mountain communities are susceptible to flood hazards [*Lenzi*, 2002; *Marion et al.*, 2004; *Comiti et al.*, 2005, 2009b] and in the context of stream restoration [*Chin et al.*, 2009].

[3] Step-pool geometry, including relationships between step length (L), step height (H_s), grain size (D), stream gradient (S), and channel width (w), and variance in these relationships, has been investigated to seek insights into formative processes, hydraulic controls, and analogies to lower-gradient systems [*Grant et al.*, 1990; *Wohl and Grodek*, 1994; *Chin*, 1999; *Chartrand and Whiting*, 2000; *Zimmermann and Church*, 2001; *Milzow et al.*, 2006; *Nickolotsky and Pavlowsky*, 2007]. Step-pool channels may have slopes of as low as 0.03 m/m [*Montgomery and Buffington*, 1997], but at gradients steeper than approximately 0.07 m/m, step-pool channels tend to have distinct morphologies, geometries, and hydraulics, with steps controlling the elevation loss (i.e., $H_s/L \sim S$) [*Church and Zimmermann*, 2007]. The ratio of step height to step length to bed gradient, $H_s/L/S$, is an often-cited measure of step geometry that illustrates the amount of elevation change created by step-pool sequences and the presence

[1]Department of Geosciences, University of Montana, Missoula, Montana, USA.
[2]Department of Geosciences, Colorado State University, Fort Collins, Colorado, USA.
[3]Faculty of Science and Technology, Free University of Bozen-Bolzano, Bolzano, Italy.
[4]Department of Land and Agro-Forest Environments, University of Padova, Legnaro, Italy.

0043-1397/11/2010WR010192

of reverse slopes between steps. *Abrahams et al.* [1995] suggest that step-pool channels are organized such that $H_s/L/S$ is typically between one and two and flow resistance is maximized, although others have documented a broader, slope-dependent range of $H_s/L/S$ [*Zimmermann and Church*, 2001; *Church and Zimmermann*, 2007]. Observations of regularity in step-pool spacing or other spatial organization have been used as evidence of hydraulic controls on step-pool formation [*Chin*, 2002; *Milzow et al.*, 2006] and of self-organization processes whereby flow resistance increases, local slope decreases, and stream power is minimized as step-pool bed forms evolve [*Chin and Phillips*, 2007].

[4] Studies of flow resistance dynamics have explored methods for prediction of roughness coefficients as a function of factors such as relative submergence (R/D_{84}) [*Lee and Ferguson*, 2002], step geometry [*Canovaro and Solari*, 2007], or unit discharge and hydraulic geometry [*Rickenmann*, 1991; *Aberle and Smart*, 2003; *Comiti et al.*, 2007; *Ferguson*, 2007; *David et al.*, 2010; *Zimmermann*, 2010], as well as partitioning of resistance between grain, spill, and other components [*Curran and Wohl*, 2003; *MacFarlane and Wohl*, 2003; *Wilcox et al.*, 2006; *Wilcox and Wohl*, 2006]. Based on flume experiments, *Wilcox et al.* [2006] conclude that the combined effects of wood and spill resistance dominate total flow resistance in step-pool channels, whereas grain resistance is relatively small. Field studies in step-pool channels have also illustrated shifts in the partitioning of resistance with discharge and the minor role of grain resistance [*MacFarlane and Wohl*, 2003; *David et al.*, 2011]. Observations of elevated sediment transport rates following an exceptional flood that destroyed steps in the Erlenbach, Switzerland, illustrate how form resistance can decrease as a result of step destruction [*Turowski et al.*, 2009]. *Zimmermann* [2010], however, suggests that stress partitioning is inappropriate for steep channels where grains actually impart form resistance, as opposed to the skin resistance associated with grains in lower-gradient systems.

[5] Step-pool hydraulics can also be evaluated in terms of the energy dissipation associated with changes in elevation and velocity head across individual step-pool sequences. For example, *Marston* [1982] calculated 12% of cumulative energy dissipation by log steps in the Oregon Coast Range, and *Hayward* [1980] calculated 93% energy dissipation by a boulder step in New Zealand. Recent efforts to quantify energy dissipation in step-pool channels [*Pasternack et al.*, 2006; *Wyrick and Pasternack*, 2008] have drawn on analyses of hydraulic jumps, stepped spillways or other hydraulic drop structures [e.g., *Moore*, 1943; *Rajaratnam and Chamani*, 1995; *Chanson*, 1994, 1996]. Flow over drops can include nappe flow, where water plunges over steps in a free falling jet, transitional flow, and skimming flow where the water surface is smoother and drops are submerged, depending on both the ratio of critical depth at the step crest (d_c) to step height (H_s) and step geometry (H_s/L) [*Chanson*, 1994]. The transition from nappe flow with jumps to transitional/skimming flow in natural stepped channels corresponds to a dramatic decrease in flow resistance and increase in velocity [*Comiti et al.*, 2009a], and skimming flow is expected to be more common in steeper ($S > 0.07$) step-pool channels during high-magnitude flood events [*Church and Zimmermann*, 2007].

[6] The observation that step-pool units produce a jet of supercritical flow over step crests that plunges into downstream pools and produces a hydraulic jump where flow transitions to subcritical [*Grant et al.*, 1990] has sparked inquiries into how jet and jump characteristics influence the morphodynamics of river steps and are in turn controlled by channel geometry [*Wyrick and Pasternack*, 2008]. Step-pool features can have submerged jets, where the flow is affected by the water surface of the downstream pool or tailwater, or free jets in which nappe flow occurs. Submerged drops can have either impinging jets, where the jet is directed toward the bed of the downstream pool, or surface jets, which are submerged in deeper pools and are therefore directed in a downstream direction rather than directly at the bed [*Wu and Rajaratnam*, 1998; *Comiti and Lenzi*, 2006; *Church and Zimmermann*, 2007].

[7] Using flume studies with a horseshoe step, *Pasternack et al.* [2006] illustrated that most of the energy dissipated as flow moves from steps to pools results from potential energy loss rather than velocity reduction, contrary to what they suggest is a common misconception regarding mountain rivers. Subsequently, *Wyrick and Pasternack* [2008] developed a model for calculating relative head loss through individual step-pool sequences in which nappe trajectory and hydraulic jump regime are key variables. This model is explained further below in the context of our study.

[8] Many of the studies discussed above have investigated possible hydraulic explanations for step-pool formation, but few of these incorporate field data on velocity and turbulence, instead relying on field measurements of step-pool geometry and/or laboratory experiments. Here we report the results of detailed measurements of three-dimensional velocities and of bed topography in a step-pool channel in the Italian Dolomites, the Rio Cordon. These data are used to investigate relationships between step architecture and hydraulics, including (1) how velocity and turbulence vary longitudinally and laterally, as a function of both flow through step-pool sequences and cross-sectional morphology; (2) energy dissipation patterns across step-pool units; and (3) feedbacks between hydraulics and morphology. Our field results are also compared to analogous hydraulics data from a step-pool stream with different hydroclimatic conditions, East St. Louis Creek in the Colorado Rockies, in order to contextualize the Rio Cordon data, to evaluate how factors such as in-stream wood influence relationships between morphology and hydraulics, and to evaluate theories for step-pool formation.

[9] The work presented here builds on a pair of field studies in East St. Louis Creek that evaluated the effect of bed form type and discharge variations on velocity and turbulence in step-pool channels, using one-dimensional measurements with a electromagnetic current meter [*Wohl and Thompson*, 2000] and three-dimensional measurements with a FlowTracker acoustic Doppler velocimeter [*Wilcox and Wohl*, 2007]. These studies documented spatial differences in turbulence intensities between steps and pools [*Wilcox and Wohl*, 2007] and suggest that higher-energy dissipation results from the wake-generated turbulence and form drag of step-pool reaches compared to the bed-generated turbulence found in more uniform gradient reaches such as runs [*Wohl and Thompson*, 2000]. We also build on the many investigations of reach-scale variability in velocity and turbulence using multidimensional measurements [e.g.,

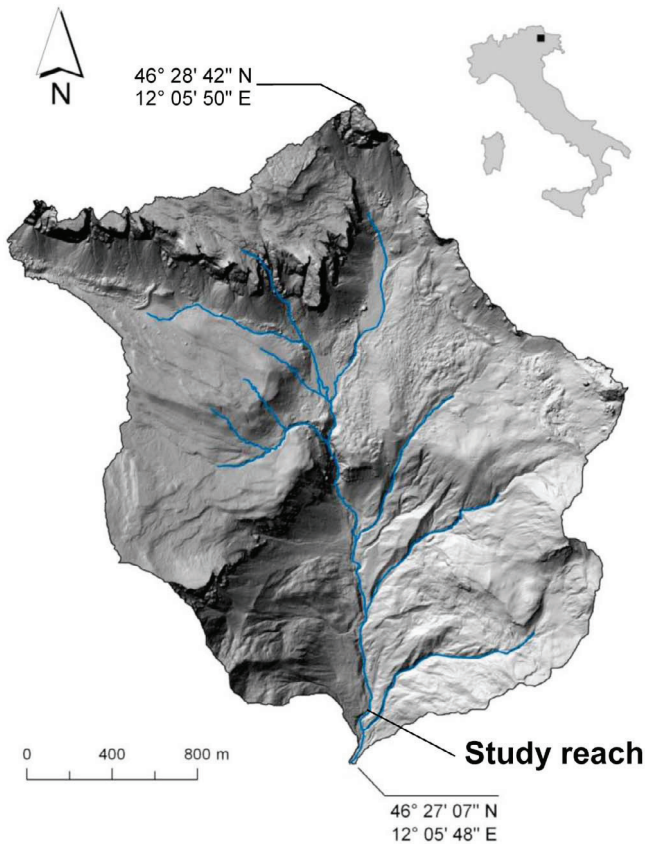

Figure 1. Hillshade digital elevation model of the Rio Cordon basin; inset shows location in Italy.

Lamarre and Roy, 2005; *Legleiter et al.*, 2007; *MacVicar and Roy*, 2007].

2. Methods

2.1. Study Area

[10] Our study area is the Rio Cordon, Italy, a step-pool channel in the eastern Italian Alps (i.e., the Dolomites) (Figure 1). Precipitation averages 1100 mm/yr, the majority of which is snow. Snowmelt generates late spring–early summer peak flows, and summer and fall thunderstorms produce many of the geomorphically effective discharges in the Rio Cordon. Water discharge, suspended sediment, and bed load fluxes have been automatically measured at intervals of less than 10 min on the Rio Cordon since 1986 [*Lenzi et al.*, 1999, 2004; *Mao et al.*, 2010]. The elevation of the study site is approximately 1800 m, with a drainage area of 5 km^2. Basin lithology consists of dolomite, volcaniclastic conglomerate, and tuffaceous sandstone.

[11] The precipitation patterns and lithology in the Cordon basin combine to create a dynamic geomorphic setting in which infrequent floods reorganize the channel. *Lenzi* [2001] documents several such events, finding that a large flood (RI >50–70 years) destabilized steps and increased sediment transport sufficiently to partially fill pools and lengthen step spacing, such that morphology transitions from step-pool to plane-bed morphology. Subsequent moderate floods then scour pools and reestablish the step sequence, resulting in an evolution toward increasing values of $H_s/L/S$ [*Lenzi*, 2001]. Other previous studies in the Rio Cordon have investigated sediment yield and transport rates [*D'Agostino and Lenzi*, 1999; *Lenzi et al.*, 2003, 2004; *Mao et al.*, 2009], incipient sediment motion [*Lenzi*, 2004; *Lenzi et al.*, 2006a; *Mao and Lenzi*, 2007], bed load travel distance [*Lenzi*, 2004], effective discharge [*Lenzi et al.*, 2006b], sediment sources [*Fontana and Marchi*, 2003], step-pool scour dynamics [*Comiti et al.*, 2005], in-stream wood [*Comiti et al.*, 2006], at-a-station hydraulic geometry [*Comiti et al.*, 2007], and automatic morphologic classification [*Trevisani et al.*, 2010].

[12] The study reach we established for measurements of flow hydraulics and bed topography in the Rio Cordon spanned 120 m, the downstream end of which was approximately 200 m upstream of the above mentioned gaging station. This reach consisted of three subreaches, each containing five distinct step-pool sequences, separated by cascade units (i.e., areas of tumbling flow without pools) (Figure 2). We consider this a step-pool reach [after *Montgomery and Buffington*, 1997], although ambiguity surrounding step-pool terminology remains [*Zimmermann et al.*, 2008; *Comiti and Mao*, 2011] and some observers would refer to this as a cascade reach containing step-pool units (which implies that steps are channel spanning) and subunits (nonspanning steps) [*Grant et al.*, 1990; *Church and Zimmermann*, 2007].

[13] The gradient steepens from 0.10 m/m in the upper two thirds of the study reach to 0.13 m/m in the downstream-most portion. Bed sediments are typically poorly imbricated, weakly rounded, and slab-like, and steps are formed by irregular transverse accumulations of boulders, many of which may have been delivered to the study reach in 1994, when a 50–70 year flood reorganized the channel [*Lenzi*, 2001; *Mao et al.*, 2009]. Median grain size in the 3 subreaches ranges from 140 to 220 mm, and the D_{84}, which is approximately representative of step-forming clasts, ranges from 410 to 480 mm. In-stream wood is absent in the study reach.

2.2. Field Measurements

[14] Topographic and hydraulics measurements were organized so as to be representative of the following positions associated with step-pool sequences: (1) steps, including positions from approximately 1 m upstream of the step crest to the crest, (2) pools (including both positions at the base of the step riser and in the zone of accelerating flow downstream of the hydraulic boil in pools), and (3) treads (areas other than steps and pools, including runs between the downstream end of the scour pool and the next step, and cascade units with tumbling flow but lacking pools) [after *Church and Zimmermann*, 2007]. In locations corresponding to steps, pools, or treads, we established 42 cross sections for topographic and velocity surveys, all of which were in our middle and downstream subreaches. Cross-section spacing around step-pool features was on the order of 1 m. Fewer and more widely spaced measurements were performed in subsections of the study reach lacking step-pool features.

[15] At approximately 0.5 m cross-channel intervals along these cross sections, a SonTek FlowTracker acoustic Doppler velocimeter (ADV) [*SonTek*, 2001; *Rehmel*, 2007] was used to measure profiles of the downstream, cross-

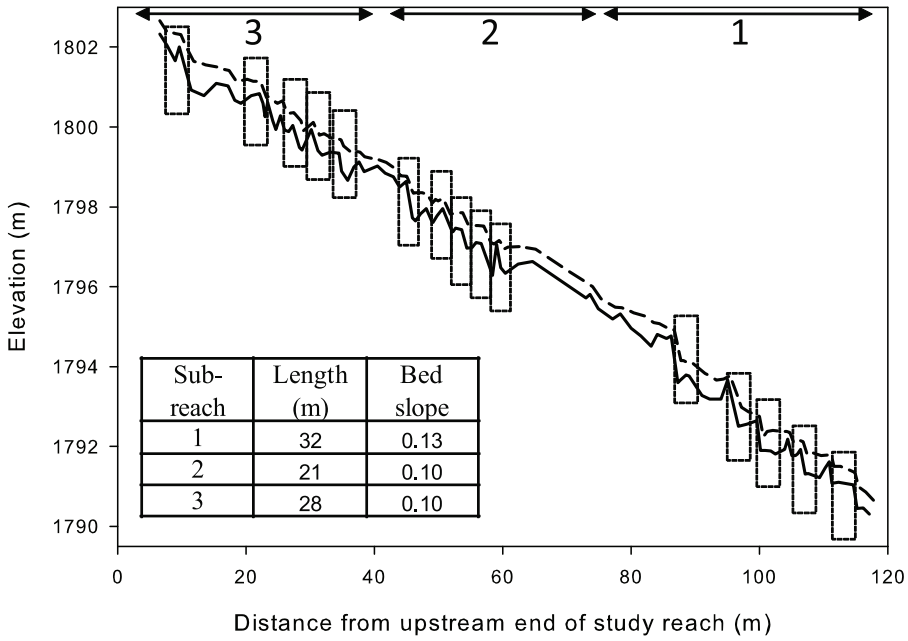

Figure 2. Longitudinal profile of thalweg (solid line) and water surface (dashed line) elevation in study reach. Numbered subreaches are delineated at top, and step-pool sequences are outlined (boxes). Additional information about step-pool geometry and hydraulics is provided in Tables 2 and 3; numbering of steps in Tables 2 and 3 is from upstream to downstream in each subreach.

stream, and vertical velocity components, which we denote as u, v, and w, respectively. To supplement cross-section-based measurements, additional velocity profiles were measured along the thalweg in the upstream subreach and at additional step and pool positions in the middle and downstream subreaches. A total of 212 velocity profiles were measured. Each velocity profile consisted of measurements at between 4 and 8 positions in the water column, at vertical intervals of 0.1 to 0.2 times the local flow depth (d). At each measurement position, a 90 s time series of three-dimensional velocities was recorded; issues associated with record length are discussed by *Buffin-Bélanger and Roy* [2005] and *Wilcox and Wohl* [2007].

[16] Because we anticipated ADV data quality issues in highly aerated and near-boundary environments, as discussed further below, we supplemented our data set by measuring velocity in selected locations using an Ott electromagnetic current meter (ECM). Electromagnetic current meters (ECMs) have been shown to perform better than ADVs in some settings [*MacVicar et al.*, 2007]. The ECM only produced information on downstream (u) velocities and at 0.2 Hz (5 s averaging), however, so did not provide multidimensional velocity data such as those provided by the FlowTracker.

[17] Bed and water surface topography were surveyed using a total station, including cross-section and longitudinal profile (water surface and thalweg) surveys, locations of ADV measurements, and grid surveys. Because measurements were guided by the location of steps, cross sections were not always perpendicular to the channel or parallel to each other. We used WinXSPro to calculate the cross-sectional flow area (A) and hydraulic radius (R) for all cross sections. Topography and velocity measurement locations for subreaches 1 and 2 are illustrated in Figure 3. These contour maps were developed in Surfer by kriging the topographic survey data, with break lines established at bankfull locations. The resulting contour maps serve as base maps onto which we overlay hydraulic data to illustrate spatial patterns, as presented below. The density of topographic data in reach 3 was insufficient to develop analogous maps in that subreach.

[18] Discharges during our surveys, which were completed in May and June 2004, ranged from 0.82 to 1.3 m^3/s (36%–57% of Q_{bf}). Field measurements were completed during a 2 week period of both considerable rainfall and spring snowmelt, resulting in intradaily and interdaily discharge fluctuations.

2.3. Analysis

2.3.1. Step Geometry Data

[19] We used our survey data to calculate several measures of step-pool geometry (Figure 4) for evaluation with respect to hydraulics measurements. These include the following: (1) step height (H_s), the change in elevation from the step crest to the deepest point of the scour pool below the step; (2) step height to base (H_b), the change in bed elevation from the step crest to the base of the step, which in some cases occurs upstream of the deepest point of the scour pool; (3) step length (L), the distance from a step crest to the crest of the next downstream step; (4) the ratio of step height to step length (H_s/L); (5) the ratio of step height/step length/bed gradient for each subreach, based on reach gradient and the average of H_s/L values [$(\overline{H_s/L})/S$]; (6) distance between the step crest and the deepest point of the downstream pool (L_{cs}), where a value of $L_{cs} = 0$ would indicate a vertical overfall from the step crest and the deepest point of the pool being directly below the step crest (i.e., $H_s = H_b$); (7) drop height (z), the elevation difference between successive step crests; and (8) residual pool depth (d_r), the difference

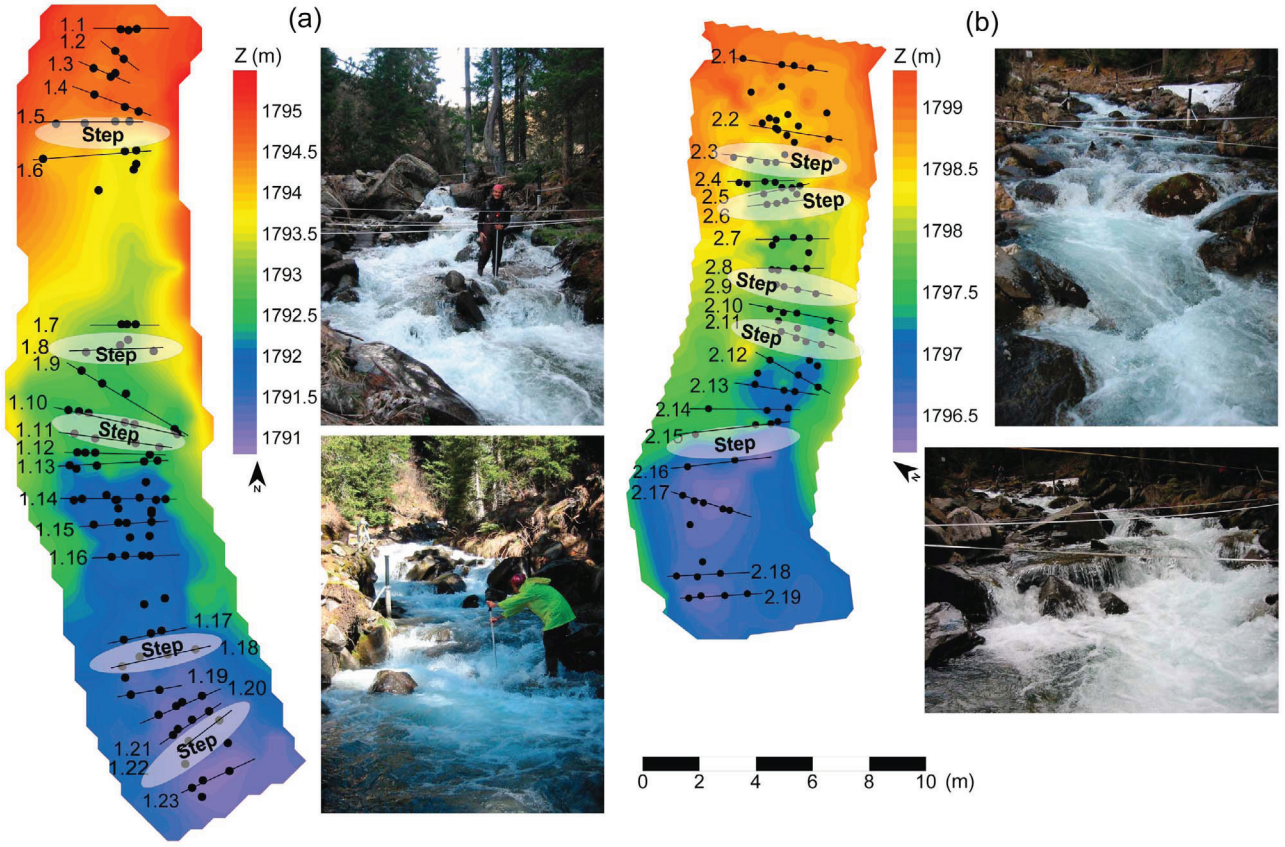

Figure 3. Contour maps of bed topography and photos of (a) subreach 1 and (b) subreach 2. Lines show location of cross sections around which velocity measurements were organized, with corresponding cross-section numbers at left. Dots represent velocity measurement locations. Top and bottom photographs illustrate upper and lower portions of each subreach, respectively.

between H_s and z, which is referred to as scour depth by some authors [e.g., *Chartrand and Whiting*, 2000].

[20] Terminology and abbreviations for step-pool geometry are variable in the published literature. Many of our metrics of step-pool geometry follow the conventions of *Church and Zimmermann* [2007], although some variables are abbreviated differently to avoid confusion with nomenclature used in energy dissipation calculations.

2.3.2. Velocity and Turbulence Data

[21] We calculated mean velocity for each velocity time series, for the u, v, and w components (U, V, and W are the

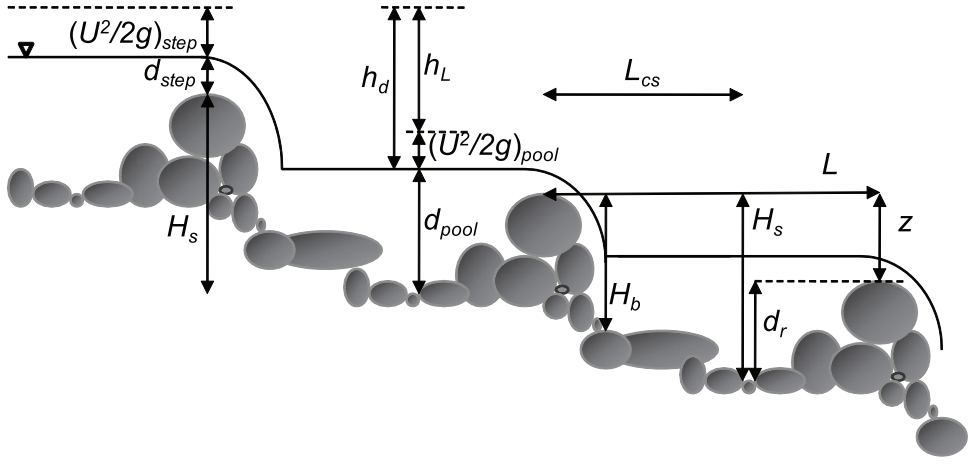

Figure 4. Sketch showing metrics of step-pool geometry and energy dissipation, modified from a combination of *Church and Zimmermann* [2007] and *Wyrick and Pasternack* [2008].

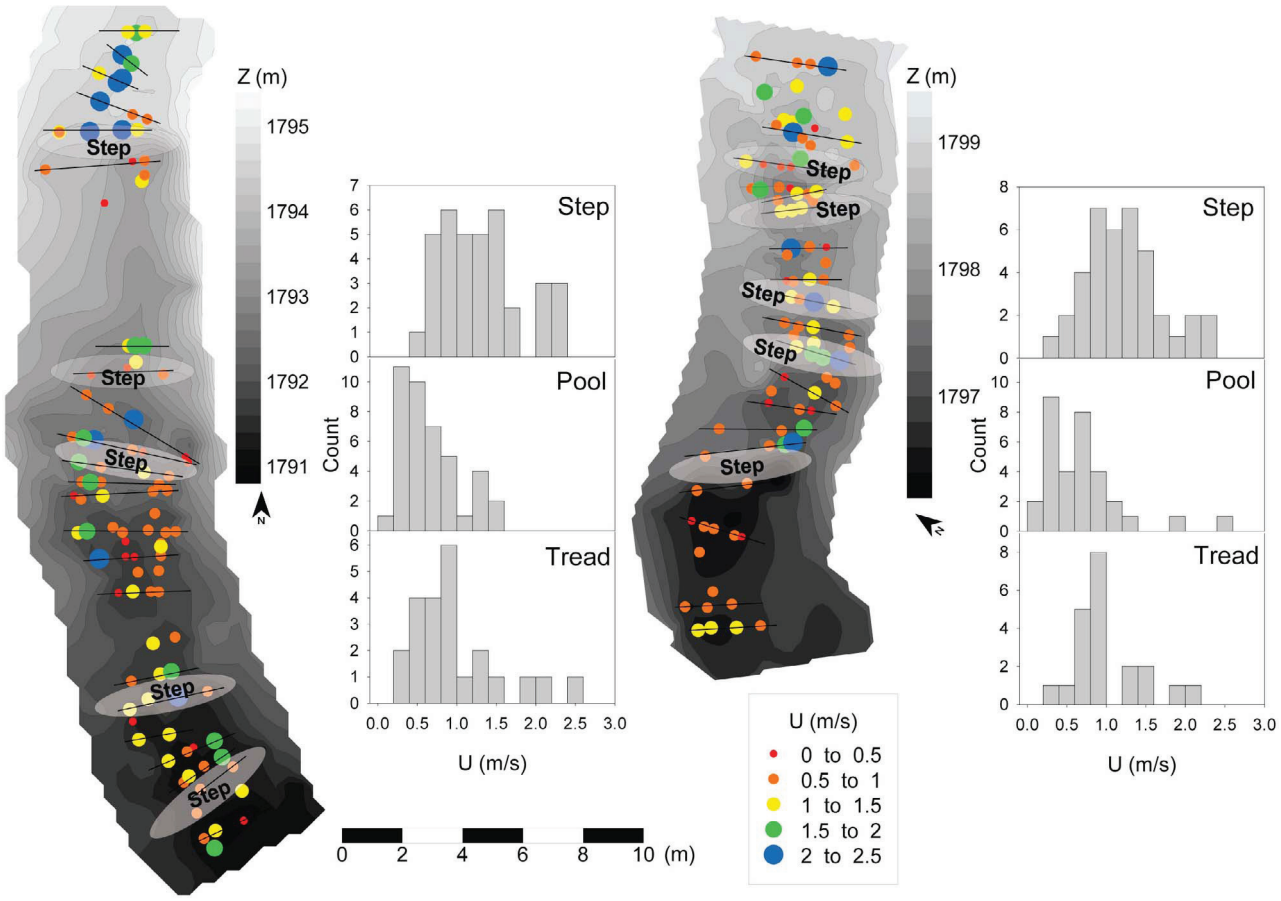

Figure 5. Spatial variation in vertically averaged downstream velocities (U, in m/s) for (left) subreach 1 and (right) subreach 2, with histograms showing U distributions in step, pool, and tread units (differences between these units are significant, $p < 0.001$). Base maps showing topography and cross-section locations are the same as in Figure 3.

mean downstream, cross-stream, and vertical velocity for a time series). We then calculated the vertically averaged velocity within each profile. Nondimensionalizing velocity measurements can facilitate comparison between study sites and discharges. For example, measured velocities can be nondimensionalized by dividing by shear velocity (u^*), a fundamental velocity scale that is most commonly determined from (1) channel slope and dimensions, $u^* = (gRS)^{0.5}$ (g is gravitational acceleration, R is hydraulic radius); (2) the logarithmic law of the wall; or (3) measured distributions of Reynolds stresses near the bed [*Nezu and Nakagawa*, 1993]. Each of these approaches is problematic for steep, rough channels such as our field area, however. The first approach assumes uniform flow and is highly sensitive to the length over which S is calculated, the second approach is based on a logarithmic velocity profile (many of our profiles are nonlogarithmic, as is typical of steep channels [*Jarrett*, 1984; *Byrd et al.*, 2000]), and the third approach requires near-bed velocity data that is beyond current measurement technologies in steep, rough channels. In light of these challenges, we present both velocities in their original, dimensioned terms and in dimensionless terms.

[22] Nondimensionalization is achieved by the first of the approaches described above:

$$U^+ = \frac{U}{u^*} = \frac{U}{\sqrt{gRS}}, \tag{1}$$

where U^+ is dimensionless downstream velocity. To calculate u^* in (1), we use R values calculated for each cross section, thereby accounting for the effect of discharge fluctuations during our field session, and reach-average values of S. The cross-stream and vertical components of velocity can be similarly nondimensionalized (producing V^+ and W^+, respectively). An additional dimensionless representation of velocity is provided by calculation of local Froude number $[U/(gd)^{0.5}]$ at each measurement location.

[23] To characterize the fluctuating components of velocity and thus turbulence, root mean squares of each velocity time series were calculated for the u, v, and w components (RMS_u, RMS_v, and RMS_w respectively) [*Clifford and French*, 1993; *Middleton and Wilcock*, 1994]. An overall turbulence intensity (TI) was calculated as the average of RMS_u, RMS_v, and RMS_w, and a dimensionless RMS was calculated for each component by dividing RMS by velocity vector magnitude (RMS_u^+, RMS_v^+, and RMS_w^+).

Table 1. Hydraulics Data, Averaged for Each Cross Section, for Subreaches 1 and 2[a]

Cross Section	Type	Q (m^3/s)	U (m/s)	V (m/s)	W (m/s)	U^+	V^+	W^+	Fr	TI (m/s)	RMS_u^+
1.1	tread	1.3	1.5	−0.1	0.1	2.5	−0.2	0.1	0.7	0.3	0.3
1.2	tread	1.3	1.9	0.0	−0.1	4.1	0.1	−0.3	1.0	0.3	0.2
1.3	tread	1.3	1.6	−0.2	0.2	3.2	−0.4	0.5	1.0	0.4	0.4
1.4	step	1.1	1.4	0.3	0.0	3.4	0.8	0.1	0.7	0.3	0.2
1.5	step	1.1	1.6	0.4	0.2	3.9	1.0	0.5	1.0	0.3	0.3
1.6	pool	1.1	0.6	−0.1	0.1	0.8	0.1	0.1	0.4	0.3	0.7
1.7	tread	1.0	1.0	0.1	0.2	1.9	0.2	0.4	0.5	0.4	0.4
1.8	step	1.0	1.1	0.0	0.2	2.1	−0.1	0.3	0.8	0.3	0.3
1.9	pool	0.9	0.5	0.1	0.1	0.8	0.2	0.2	0.5	0.4	0.9
1.10	tread	0.9	0.8	0.1	0.1	1.4	0.2	0.2	0.5	0.2	0.6
1.11	step	0.9	1.0	0.1	0.0	1.6	0.1	0.0	0.5	0.2	0.3
1.12	pool	0.8	1.1	0.2	0.0	1.9	0.4	0.0	0.7	0.3	0.3
1.13	pool	0.8	0.8	0.1	0.1	1.5	0.1	0.2	0.6	0.2	0.4
1.14	pool	0.8	0.7	0.0	0.1	1.1	0.0	0.1	0.5	0.3	0.5
1.15	tread	0.8	0.7	0.0	0.0	1.0	0.0	0.0	0.4	0.2	0.5
1.16	tread	0.8	0.7	0.0	0.1	1.3	0.1	0.1	0.4	0.2	0.3
1.17	step	0.9	1.0	0.1	0.0	1.8	0.2	0.1	0.6	0.3	0.3
1.18	step	0.8	1.2	0.0	−0.1	2.4	0.0	−0.3	0.7	0.2	0.3
1.19	pool	0.9	1.4	0.0	−0.1	2.9	−0.1	−0.2	0.9	0.3	0.4
1.20	pool	0.9	0.6	0.0	0.2	1.0	0.0	0.3	0.3	0.2	0.6
1.21	tread	1.0	0.6	0.3	0.0	1.0	0.5	0.1	0.3	0.3	0.4
1.22	step	1.0	1.0	0.1	0.1	1.9	0.2	0.2	0.6	0.3	0.4
1.23	pool	1.0	0.9	−0.1	0.1	1.5	−0.1	0.2	0.5	0.4	0.5
2.1	tread	1.0	1.2	0.1	−0.1	2.8	0.1	−0.3	0.8	0.2	0.3
2.2	step	0.9	1.3	0.0	0.0	3.0	0.0	0.0	0.9	0.2	0.4
2.3	step	1.0	1.1	−0.1	0.1	2.4	−0.1	0.3	0.8	0.3	0.4
2.4	pool	0.9	0.5	-	-	0.9	-	-	0.2	-	-
2.5	tread	1.0	0.9	0.0	0.2	1.4	0.0	0.3	0.4	0.3	0.5
2.6	step	1.0	1.1	0.2	0.2	1.8	0.2	0.3	0.6	0.3	0.3
2.7	pool	1.1	0.6	0.1	0.2	1.3	0.1	0.5	0.5	0.3	0.5
2.8	tread	1.1	0.7	0.0	0.2	1.7	0.0	0.6	0.3	0.3	0.5
2.9	step	1.1	1.4	0.1	0.0	3.2	0.3	0.0	0.9	0.2	0.2
2.10	pool	1.0	0.7	0.0	0.2	1.4	0.0	0.4	0.4	0.4	0.5
2.11	step	1.0	1.1	0.0	0.2	2.5	−0.1	0.3	0.6	0.3	0.5
2.12	pool	1.0	0.6	0.0	0.2	1.1	−0.1	0.3	0.3	0.5	0.7
2.13	tread	0.9	0.4	0.0	0.1	0.7	0.0	0.1	0.2	0.3	0.8
2.14	tread	0.9	0.3	−0.1	0.2	0.5	0.0	0.2	0.4	0.3	0.8
2.15	step	1.0	1.3	−0.1	−0.1	3.3	−0.4	−0.1	0.9	0.5	0.6
2.16	pool	1.0	0.6	-	-	1.0	-	-	0.5	-	-
2.17	pool	1.0	0.5	0.2	0.1	0.9	0.3	0.2	0.2	0.3	0.6
2.18	tread	1.0	0.8	0.2	0.0	1.7	0.5	0.1	0.4	0.2	0.3
2.19	step	1.0	1.2	0.4	−0.1	2.7	0.9	−0.2	0.8	0.2	0.2

[a]Values shown as 0.0 are rounded from within ±0.05; cells shown as "-" indicate that no data were retained after filtering for the given parameter.

Vertical averages of these values were calculated for each profile, similarly as for mean velocities, and were then used to evaluate longitudinal and lateral variations in hydraulics. Although the 1 Hz frequency of the FlowTracker ADV is inadequate for detailed turbulence analysis, the RMS values provide an approximate measure of turbulence intensities and facilitate comparisons.

[24] Velocities measured using acoustic methods are subject to errors as a result of factors including air bubbles in the flow [*Rodriguez et al.*, 1999], aliasing [*Goring and Nikora*, 2002]; and Doppler noise [*Nikora and Goring*, 1998], among other factors [*MacVicar et al.*, 2007; *Rehmel*, 2007]. These problems are especially acute in steep, aerated channels with shallow depths and rough beds [*Vallé and Pasternack*, 2002; *Wilcox and Wohl*, 2007], posing challenges for multidimensional velocity and turbulence measurements and precluding the use of higher-frequency ADVs used in hydraulics studies in larger, lower-gradient streams and laboratories (see overview by *Buffin-Bélanger and Roy* [2005]).

[25] Extensive filtering of FlowTracker data was therefore required to address limitations on ADV performance in the Rio Cordon [*Wilcox and Wohl*, 2007]. First, we removed 1 s velocity measurements with signal-to-noise ratio (SNR) <10 dB, the manufacturer's lower recommended limit for optimal operating conditions [*SonTek*, 2001]. SNR measures the strength of the reflected acoustic signal compared to instrument noise for each velocity reading and is reported by the instrument as an indicator of data quality [*SonTek*, 2001]. Next, spikes were removed, where spikes are defined as data points >3 standard deviations away from the time series mean calculated after SNR filtering. Each time series was then plotted and individual data points (or entire time series) that appeared to represent aliasing or other noise were removed. For example, time series with large scatter and near-zero means in the downstream component were typically assumed to represent noise and were eliminated. Finally, we eliminated time series with fewer than 60 data points remaining after filtering and time series with $RMS^+ > 2$. The same basic filtering approach was employed by *Wilcox and Wohl* [2007] and is described further therein. After elimination of ADV profiles using these filtering steps and substitution with ECM data where available, ECM measurements accounted for 18% of our velocity data set. As a further means of evaluating ADV and ECM measurements, we also back calculated the average velocity along each cross

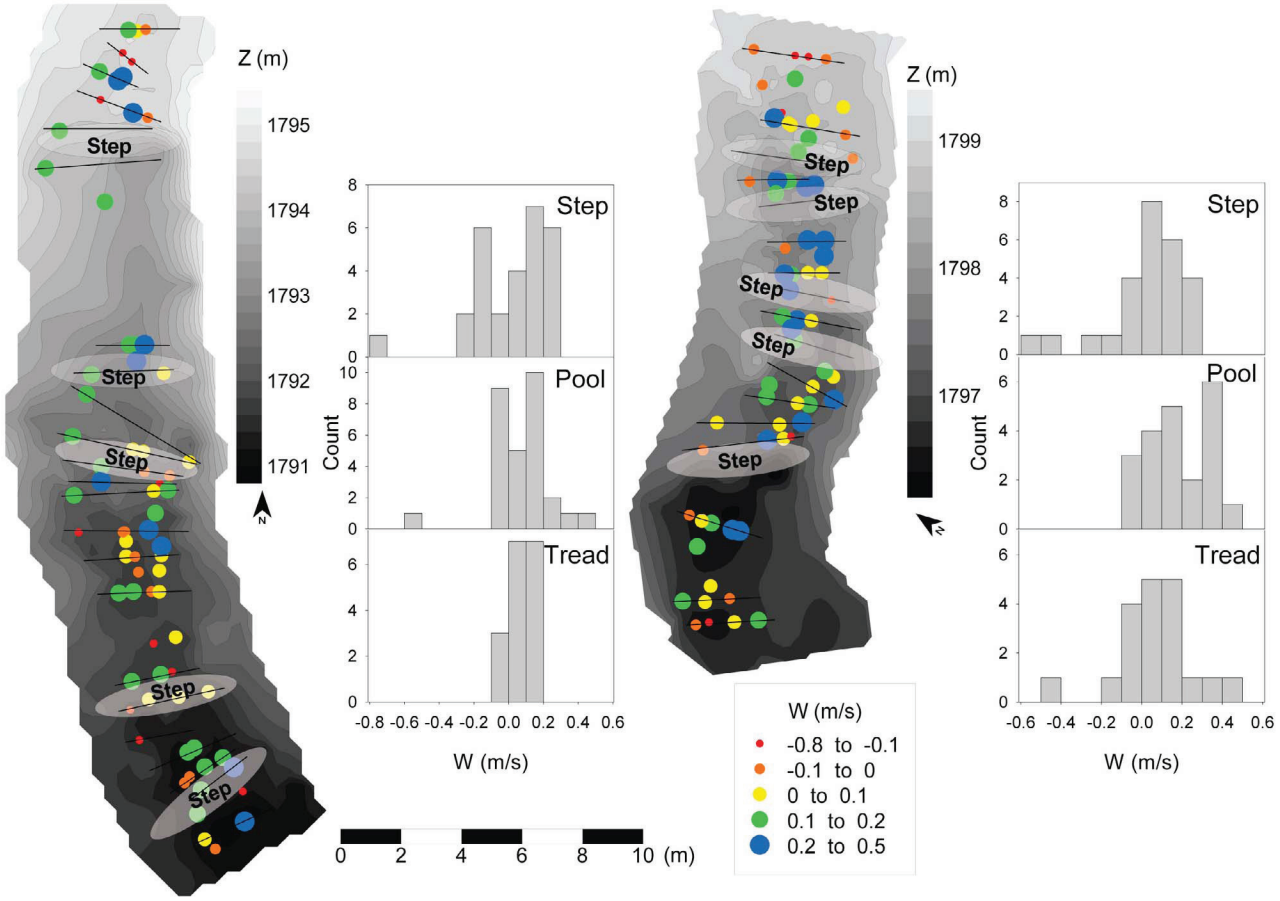

Figure 6. Spatial variation in vertically averaged vertical velocities (W, in m/s) for (left) subreach 1 and (right) subreach 2, with histograms showing W distributions in step, pool, and tread units (differences between these units are marginally significant, $p = 0.04$). Positive values denote flow away from the bed, and negative values indicate flow toward the bed. Base maps showing topography and cross-section locations are the same as in Figure 3.

section by continuity, combining discharge data from the downstream gaging station and surveyed cross-sectional flow areas.

2.3.3. Energy Dissipation

[26] We calculated energy dissipation associated with step-pool sequences using the general energy equation with modifications to account for jump submergence, following methods developed for studying natural hydraulic jumps in mountain channels [*Pasternack et al.*, 2006; *Wyrick and Pasternack*, 2008]. The general energy equation expresses flow energy between any two sections of channel as follows:

$$\left[Z_{up} + d_{up} + \left(\frac{\alpha U^2}{2g}\right)_{up}\right] = \left[Z_{down} + d_{down} + \left(\frac{\alpha U^2}{2g}\right)_{down}\right] + h_L, \quad (2)$$

where the subscripts "up" and "down" refer to upstream and downstream sections, respectively, Z is bed elevation, d is flow depth, $\alpha U^2/2g$ is velocity head, which represents kinetic energy from fluid motion and α is a coefficient that accounts for velocity variations across a section, and h_L is head loss, which represents energy dissipation as a result of the conversion of mechanical energy to heat [*Henderson*, 1966; *Roberson and Crowe*, 1997]. The energy coefficient α in (2) is often assumed to equal one, which implies that velocities do not vary across the section. If α is similar at upstream and downstream sections, it can be neglected in calculation of h_L.

[27] Equation (2) can be applied to calculation of energy dissipation through step-pool sequences, taking into account the degree of hydraulic jump submergence. Submergence occurs when the tailwater (pool) depth is high enough to affect flow over the crest [*Wu and Rajaratnam*, 1996] and the jump is upstream of the break in the water surface slope produced by plunging flow from the upstream step [*Leutheusser and Birk*, 1991; *Wyrick and Pasternack*, 2008]. With slight variations from the notation of *Pasternack et al.* [2006] and *Wyrick and Pasternack* [2008], the energy equation (2) can thus be expressed as follows:

$$E_{step} = H + H_s = h_d + d_{pool} = E_{pool} + h_L, \quad (3)$$

where the subscripts "up" and "down" in (2) are replaced with "step" and "pool," denoting locations at the step crest and in the pool downstream, respectively; E_{step} and E_{pool} are total energy at the step crest and in the pool downstream, respectively; H is specific energy (velocity head plus flow depth) at the step crest;

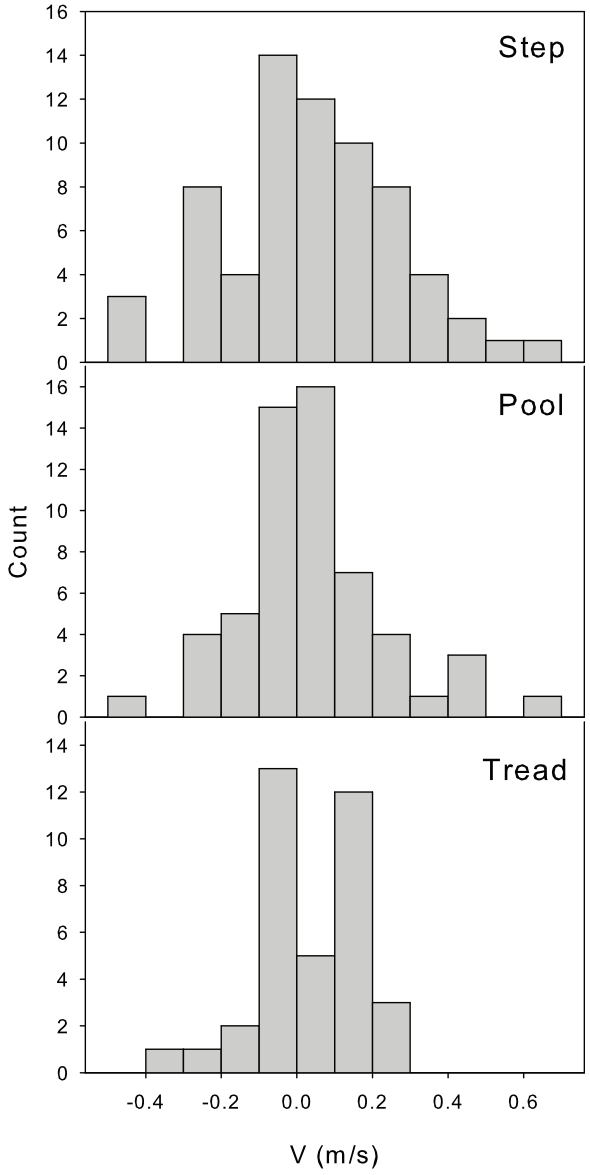

Figure 7. Distributions of vertically averaged cross-stream velocities (V, in m/s) in step, pool, and tread units (differences between these units are not significant, $p = 0.13$). Positive values denote flow toward the left bank, and negative values indicate flow toward the right bank.

H_s (step height) is equal to $Z_{step} - Z_{pool}$; and h_d is a submergence variable equal to h_L plus downstream (pool) velocity head (Figure 4). Where hydraulic jumps are not submerged, energy loss (h_L) is simply $E_{step} - E_{pool}$. For the case of a fully submerged jump, the velocity head at the downstream location represents the head loss, as is evident by rearrangement of (3) [*Wyrick and Pasternack*, 2008].

[28] Energy loss (h_L) can be nondimensionalized to provide a measure of fractional energy dissipation (i.e., relative head loss):

$$\frac{h_L}{H + H_S}. \tag{4}$$

Energy on the upstream side of the step can be nondimensionalized as well, where $(H + H_s)/H$ represents dimensionless upstream energy and incorporates information about both discharge and step height. Submergence can be nondimensionalized as h_d/H, which is indicative of the hydraulic jump regime [*Wyrick and Pasternack*, 2008].

[29] These calculations were performed for each step-pool sequence in subreaches 1 and 2 in order to evaluate energy dissipation patterns, using velocity measurements to calculate cross-section-averaged velocity, cross-section surveys to calculate wetted width at the time of surveys, and back-calculated flow depths from continuity. To evaluate the sensitivity of energy dissipation calculations to variations in α, we calculated α for several of our cross sections, as the average of cubed velocities for subsections of the channel divided by the cube of the cross-section-averaged velocity [*Dingman*, 2009].

3. Results

[30] To illustrate the relationship between the morphology of step-pool structures and hydraulics, vertically averaged downstream (U) velocities at each measurement point are overlain on TINs representing the bed topography of subreaches 1 and 2, with accompanying histograms of velocity distributions for each morphology type (Figure 5). Hydraulics data are summarized in Table 1 as well. As is expected and intuitive, a general pattern of flow acceleration toward and over step crests and deceleration as it plunges into pools was present. Downstream velocities were highest above steps, where, across all step measurements locations, they averaged 1.2 (±0.47) m/s ($U^+ = 2.5 \pm 1.2$), and lowest in pools ($U = 0.68 \pm 0.42$ m/s; $U^+ = 1.1 \pm 0.7$); tread locations were intermediate ($U = 1.0 \pm 0.50$ m/s; $U^+ = 1.8 \pm 0.97$). Analysis of variance (ANOVA) indicates that these differences are significant ($p < 0.001$ for both U and U^+).

[31] Vertical (W) velocities were highest in pools ($W = 0.12 \pm 0.17$ m/s; $W^+ = 0.22 \pm 0.28$, where positive values denote upward flow moving away from the bed), with marginally significant differences between bed form types ($p = 0.04$ for both W and W^+). Negative W values, indicating flow toward the bed, were most commonly found in treads and areas approaching steps, whereas positive W values were most common in pools (Figure 6). Cross-stream (V) velocities did not show consistent patterns with morphology type ($p = 0.13$ for variation between step, pool, and tread positions; Figure 7), however, and are not plotted over contour base maps as for U and W components. Locally high V values occurred where oblique steps produced lateral flow. Turbulence intensities did not vary between morphology types either (Figure 8; for TI, $p = 0.43$; for RMS_u^+, $p = 0.13$), contrary to our expectation that pools would have higher TI values.

[32] As comparison between the magnitudes of the U and W components indicates (Figures 5 and 6 and Table 1), velocities were dominated by the downstream component but vertical flow away from the bed was evident in pools, as a result of impinging jets and roller eddies. The magnitudes of downstream (U) and vertical (W) velocity components were uncorrelated in pools or elsewhere, such that lower downstream velocities did not necessarily correlate with stronger vertical flow components.

[33] Although the histograms in Figure 5 and the ANOVA show clear differences in downstream velocities between steps, pools, and treads, patterns of velocity differences

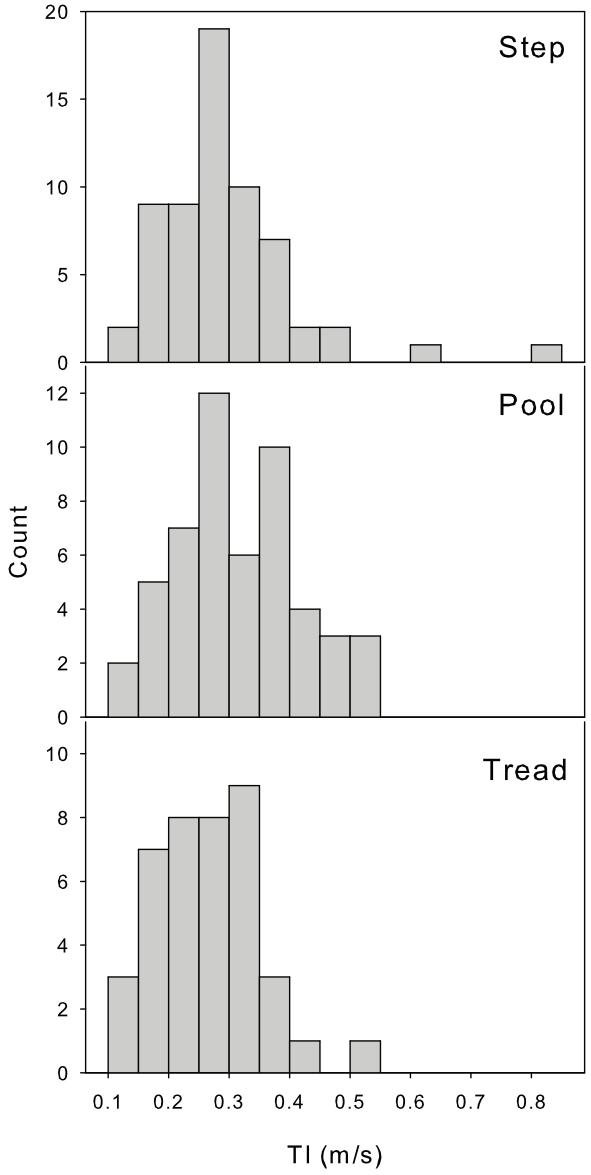

Figure 8. Distributions of vertically averaged turbulence intensities (TI) in step, pool, and tread units (differences between these units are not significant, $p = 0.43$). Turbulence intensity is calculated as the average of RMS_u, RMS_v, and RMS_w components.

between step and pool locations are obscured by lateral variations in velocity along a given cross section on a step crest or in a pool. The lateral arrangement of most steps differed from an idealized step that spans the channel perpendicular to the banks and at a consistent elevation, producing critical depth at the crest and damming of the upstream tread and pool ("ponded" steps). Instead, many steps were what we refer to as "leaky," with cross-stream variability in the topography of step crests as a result of the arrangement of boulder accumulations and/or gaps between boulders in step crests (e.g., Figure 9). Likewise, many pools had flattened boulders mantling portions of their bed, causing cross-channel variations in pool depth. These morphologic variations in turn produced considerable variability in velocity and turbulence, as well as in the associated spill resistance, energy dissipation and jet characteristics, of the

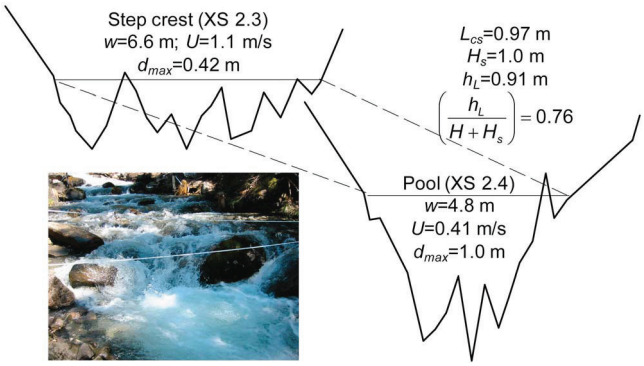

Figure 9. Cross-section geometry across a "leaky" step-pool sequence (reach 2, step 1). Plots have 4X vertical exaggeration and use consistent scaling with each other, although distance between sections is exaggerated. Horizontal lines across each cross section are drawn as to connect surveyed water's edge locations on the left and right banks. Actual water surface was typically not horizontal, however, as is evident in the inset photograph of the step-pool sequence plotted here.

flow traveling into the downstream pool. Variability in pool velocities as a result of the morphologic variations described above was especially marked, with high-velocity jets through pools exceeding 1 m/s but modes of pool velocities <0.5 m/s (Figure 5). Energy coefficients (α), which provide a measure of lateral variations in velocity along cross sections, averaged 1.5 for a subset of our cross sections, with no

Table 2. Step Geometry Data for Subreaches 1–3, Calculated From Longitudinal Profile Survey[a]

Step	H_b (m)	H_s (m)	L (m)	H_s/L	L_{cs} (m)	z (m)	d_r (m)
Reach 1							
1	1.18	1.59	8.80	0.18	1.05	1.11	0.48
2	1.16	1.16	4.51	0.26	1.67	1.01	0.15
3	0.75	0.84	4.81	0.17	0.61	0.47	0.37
4	0.61	0.71	4.47	0.16	0.73	0.31	0.40
5	0.54	0.54	3.79	0.14	0.36	0.51	0.03
Mean	0.85	0.97	5.28	0.18	0.88	0.68	0.29
Reach 2							
1	0.91	1.00	3.13	0.32	0.97	0.69	0.31
2	0.50	0.58	2.93	0.20	1.24	0.49	0.09
3	0.46	0.46	3.06	0.15	0.84	0.33	0.13
4	0.50	0.80	2.40	0.33	1.11	0.03	0.77
5	0.58	0.72	5.61	0.13	0.67	0.42	0.30
Mean	0.59	0.71	3.43	0.23	0.97	0.39	0.32
Reach 3							
1	0.46	0.69	3.15	0.22	0.41	0.23	0.46
2	0.53	0.65	4.28	0.15	1.00	0.59	0.06
3	0.56	0.62	2.87	0.22	1.03	0.10	0.52
4	0.24	0.57	1.25	0.46	0.54	0.21	0.36
5	1.08	1.22	7.64	0.16	1.83	0.91	0.31
Mean	0.57	0.75	3.84	0.24	0.96	0.41	0.34
Grand mean	0.67	0.81	4.18	0.22	0.94	0.49	0.32
Standard deviation	0.28	0.31	1.97	0.09	0.42	0.32	0.20
Maximum	1.18	1.59	8.80	0.46	1.83	1.11	0.77
Minimum	0.24	0.46	1.25	0.13	0.36	0.03	0.03

[a]Steps are shown in Figure 2, and metrics are illustrated in Figure 4. Variables are as follows: H_b, step height, measured from step crest to step base; H_s, step height, measured from step crest to pool bottom; L, step length; L_{cs}, distance from step crest to pool bottom; z, drop height, the elevation difference between successive step crests; d_r, residual pool depth ($H_s - z$).

Table 3. Energy Dissipation Calculations, Where Values Calculated "Upstream" and "Downstream" are for Cross Sections Measured Along Step Crests and in the Pool Below Each Step, Respectively[a]

			Upstream (Step Crest)							Downstream (Pool)									
Step	Q (m^3/s)	H_s (m)	d_{step} (m)	w_{step} (m)	U_{step} (m/s)	$(U^2/2g)_{step}$ (m)	H (m)	E_{step} (m)	$(H + H_s)/H$	d_{pool} (m)	d_{pool}/H	w_{pool} (m)	U_{pool} (m/s)	$(U^2/2g)_{pool}$ (m)	H_{pool} (m)	h_d (m)	h_d/H	h_L (m)	$h_L/(H + H_s)$
Reach 1																			
1	1.1	1.59	0.19	4.2	1.39	0.10	0.29	1.9	6.5	0.40	1.4	4.9	0.57	0.02	0.41	1.5	5.1	1.47	0.78
2	0.96	1.16	0.17	5.0	1.12	0.06	0.23	1.4	6.0	0.40	1.7	5.1	0.46	0.01	0.41	0.99	4.2	0.98	0.70
3	0.83	0.84	0.24	4.5	0.78	0.03	0.27	1.1	4.1	0.27	1.0	4.2	0.73	0.03	0.30	0.84	3.1	0.81	0.73
4	0.86	0.71	0.20	3.3	1.29	0.08	0.29	1.0	3.5	0.33	1.1	4.3	0.60	0.02	0.35	0.67	2.3	0.65	0.65
5	1.0	0.54	0.25	3.9	1.03	0.05	0.31	0.8	2.8	0.25	0.8	4.7	0.85	0.04	0.29	0.60	1.9	0.56	0.66
Reach 2																			
1	0.97	1.00	0.13	6.6	1.13	0.07	0.20	1.2	6.1	0.24	1.2	4.4	0.93	0.04	0.28	0.96	4.9	0.91	0.76
2	1.0	0.34	0.28	3.4	1.10	0.06	0.35	0.7	2.0	0.42	1.2	4.2	0.61	0.02	0.43	0.27	0.8	0.25	0.37
3	1.1	0.58	0.26	3.0	1.37	0.10	0.35	0.9	2.7	0.28	0.8	5.2	0.73	0.03	0.31	0.65	1.9	0.62	0.67
4	1.0	0.46	0.17	5.6	1.10	0.06	0.23	0.7	3.0	0.29	1.2	5.6	0.64	0.02	0.31	0.40	1.7	0.38	0.55
5	0.97	0.80	0.14	5.5	1.28	0.08	0.22	1.0	4.6	0.44	2.0	3.9	0.56	0.02	0.45	0.58	2.6	0.57	0.56

[a]Variables are as follows: Q, discharge at the time of measurements; H_s, step height; d, flow depth; w, wetted width; U, cross section average velocity; $U^2/2g$, velocity head; H, specific energy (depth plus velocity head); E, total energy; $(H + H_s)/H$, dimensionless energy; d_{pool}/H, relative depth; h_d, submergence; h_d/H, relative submergence; h_L, head loss; $h_L/(H + H_s)$, relative head.

systematic differences between steps and pools, and were deemed to be sufficiently similar to justify neglecting them in the energy dissipation calculations (equation (2)) presented below.

[34] To further evaluate hydraulic relationships to morphology, we calculated metrics describing the geometry of each step-pool sequence in our study reach (Table 2). Average step height (H_s) was 0.67 ± 0.28 m and average step length (L) was 4.2 ± 2.0 m, resulting in average H_s/L of 0.22 ± 0.09. Reach 1 had both the highest and longest steps, resulting in a slightly lower H_s/L than in the other subreaches (Table 1). Reach 1 also had the lowest $(\overline{H_s/L})/S$, 1.5, versus $(\overline{H_s/L})/S$ values of 2.3 and 2.4 in subreaches 2 and 3, respectively. Average distance from crest to base (L_{cs}) was 0.94 ± 0.42 m. Average residual pool depth was 0.32 ± 0.20 m, although several pools were very poorly developed, with residual depths less than 0.15 m, as a result of boulders mantling the pool bottom and inhibiting scour. No consistent pattern of either contractions or constrictions of the channel between step crests and pools was observed, and width changes between steps and pools were not related to step height (r^2 = 0.05).

[35] Calculations of fractional energy dissipation (equation (3)) showed that step-pool sequences in our study reach dissipate an average of approximately two thirds of the energy as flow moves from the step crest to the downstream pool (mean of relative head loss = 0.64 ± 0.12; range = 0.37–0.78 for individual step-pool sequences; Table 3). At the low end of the energy dissipation values was step 2 in reach 2 (0.37), the lowest step in our study reach and one that, instead of a distinct overfall, descended from step crest to pool as a ramp (L_{cs} = 1.24 m). Most head loss from steps to pools resulted from elevation changes (potential energy loss) rather than velocity reduction. Specific energy increased across many of our step-pool units (i.e., the increase in flow depths from step crest to pool was greater than the reduction in velocity head; Table 3), but a positive energy grade line ($E_{up} > E_{down}$) was maintained.

[36] The spatial pattern of measured Froude numbers in our study reaches also illustrates variations in flow regime (Figure 10). Froude numbers exceeded 1 (i.e., supercritical flow) at only a few locations, all of which are either at or approaching step crests. In some cases, supercritical flow that we observed at step crests could not be measured because flow depths were too small for ADV measurements, but typically supercritical flow did not spread across the entire step crest because of the geometric irregularities discussed above. All nonstep measurement locations had subcritical flow.

[37] Figure 11 shows dimensionless upstream energy versus dimensionless submergence for Cordon steps, along with lines differentiating jump regimes [*U.S. Bureau of Reclamation*, 1948; *Wyrick and Pasternack*, 2008]. This illustrates that our steps are divided approximately equally between classic hydraulic jumps, where the jump occurs near the base of the step, and pushed-off jumps where the jump is found downstream from the base. These differing jump regimes reflect the morphology of the step-pool sequence; steps in which flow tumbles over boulders without a single, distinct vertical drop produced sloping jets and pushed-off jumps. None of the steps plot above the top curve, which represents the threshold above which supercritical flow persists through the step-pool sequence, without a hydraulic jump, a result that is consistent with calculated Froude numbers below one in all pool locations (Figures 10 and 11). Nor do any steps plot in the drowned jump regime, which represents "submerged jumps with a strong upstream recirculation" [*Wyrick and Pasternack*, 2008, paragraph 33]. Although some individual time series of velocity measurements included negative U values in pools, indicative of upstream flow, widespread evidence of upstream recirculation was not observed in our velocity data.

4. Discussion

4.1. Feedbacks Between Hydraulics and Morphology

[38] Feedbacks between hydraulics and morphology are evident at scales of individual step-pool units, sequences of steps and pools, and along cross sections. At the scale of individual step-pool units, hydraulics reflect step height, the arrangement and shape of bed particles both in the step crest and below the step, and pool shape. Many steps in the Rio Cordon, rather than forming a consistent "drop structure" of clasts across the channel, are nonlinear and/or oblique to the flow, produce what has been referred to as nappe interfer-

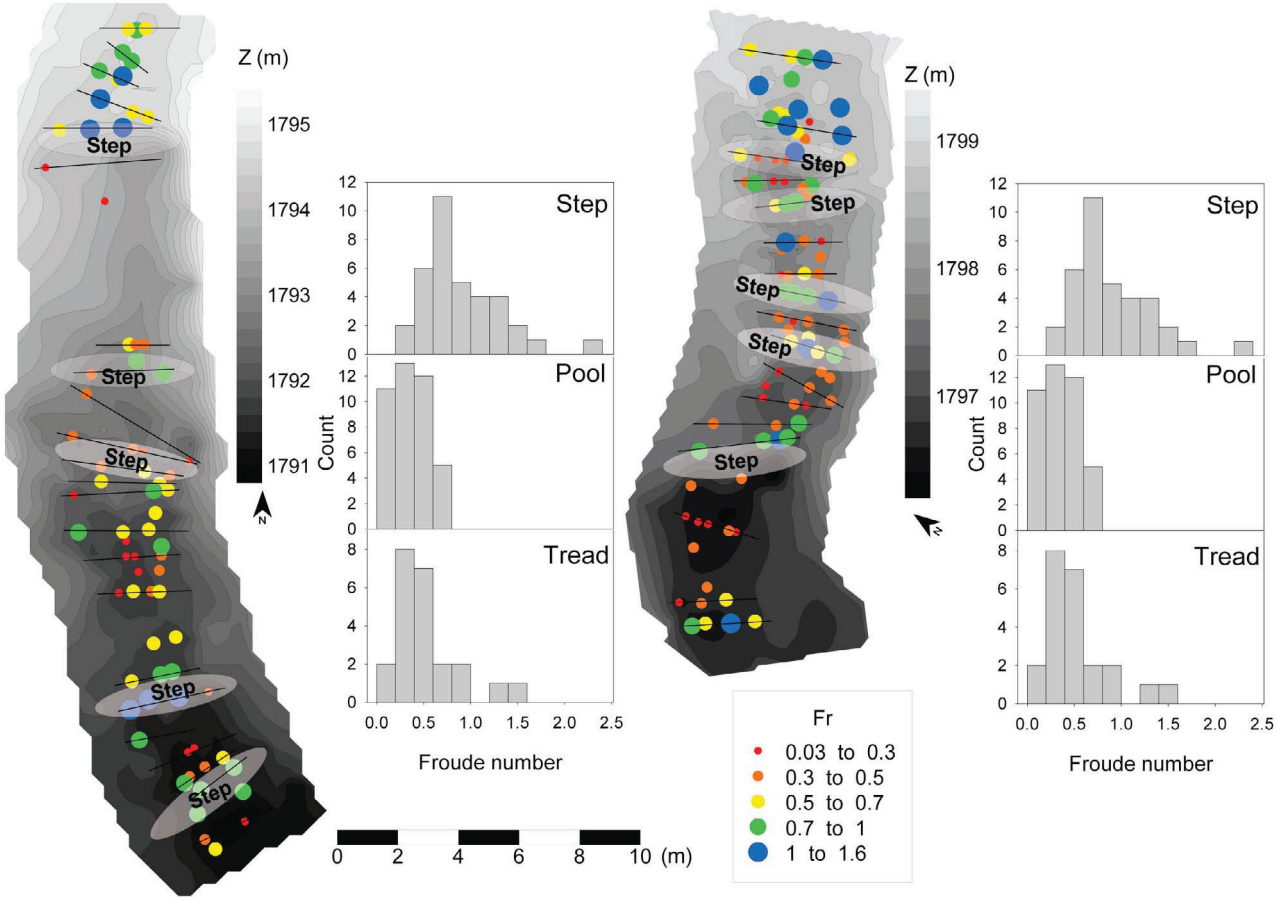

Figure 10. Spatial variation in Froude number for (left) subreach 1 and (right) subreach 2, with histograms showing *Fr* distributions in step, pool, and tread units. Both supercritical ($Fr > 1$) and subcritical ($Fr < 1$) are found in step and tread positions, but flow is exclusively subcritical in all pool positions. Base maps showing topography and cross-section locations are the same as in Figure 3.

ence [*Marion et al.*, 2004; *Wyrick and Pasternack*, 2008], and have gaps through which high-velocity jets pass into downstream pools (e.g., Figure 9). Lateral variation in the morphology and hydraulics of step crests appears to produce a feedback whereby high velocities are maintained through step-pool sequences, flow resistance is smaller compared to the case of spanning steps that dam the flow, and high transport capacities reduce the likelihood that clasts will be deposited to fill gaps in steps. Lateral and longitudinal variations are therefore coupled. In addition, some steps are oblique to the banks, setting up lateral flow components and directing stresses toward banks rather than toward downstream pools.

[39] Flume experiments have suggested that differences in step configurations, such as tranverse versus oblique planforms, are attributable to stream power variations [*Weichert et al.*, 2008]. We observed substantial architectural variability in step-pool sequences exposed to similar stream powers (i.e., within the same subreach), however, suggesting that random local factors (e.g., protruding boulders from the banks, partial step failures from toe erosion) promote such variability.

[40] Feedbacks also arise from particle shape, which affects imbrication, protrusion, and mobility. Many boulders in

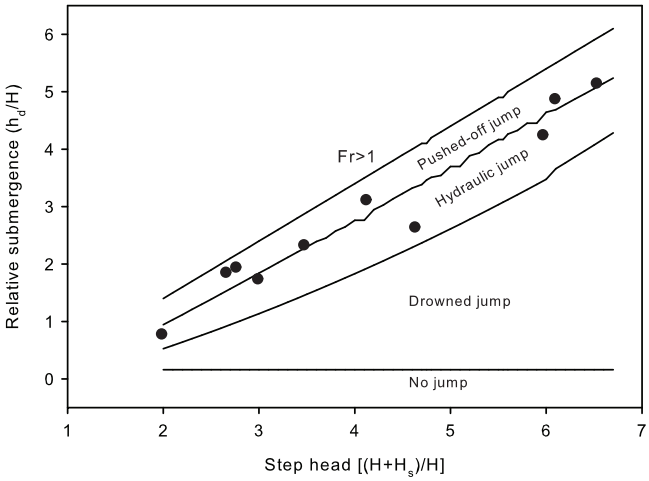

Figure 11. Dimensionless upstream energy (step head) versus dimensionless (relative) submergence for Cordon steps, with lines differentiating jump regimes.

Table 4. Comparison of Step-Pool Study Sites in Rio Cordon, Italy, and East St. Louis Creek, Colorado

	Cordon	East St. Louis
Precipitation (mm/yr)	1100	700
Drainage area (km^2)	5	8
Reach gradient	0.12	0.10
Elevation (m)	1800	2920
Geology	dolomite, volcaniclastic conglomerate, tuffaceous sandstone	gneiss, schist, granitic
Grain size D_{50} (mm)	170	78
Grain size D_{84} (mm)	410–480	260
Channel width (m)	5–6	4

the Cordon are slab-like and flattened (Figures 3 and 9). As step formers, such boulders produce lower frontal area and associated drag and damming of the flow than rounded clasts. Slabby boulders also often mantle the bed of pools as well, limiting scour. Pool scour often only occurs further downstream of the step, beyond the impingement point of the step's jet, where sediment is finer, resulting in the L_{cs} values cited above. Many of the Cordon boulders appear poorly imbricated and unstable, based on their instability underfoot.

[41] Although our study focuses on spatial aspects of relationships between step-pool morphology and hydraulics, the nature and strength of feedbacks likely varies temporally as well, as a function both of discharge [*Wilcox and Wohl*, 2007; *Wyrick and Pasternack*, 2008; *Comiti et al.*, 2009a] and of time since channel-altering floods and subsequent channel evolution. As discharge increases and bed forms become increasingly submerged, flow resistance decreases, hydraulics become less sensitive to bed irregularities [*Wilcox and Wohl*, 2006; *Comiti et al.*, 2009a], and a transition from impinging jets and nappe flow to surface jets and/or skimming flow occurs. Large floods (or debris flows [*Gintz et al.*, 1996]) can remove steps by mobilization of step-forming clasts or by downstream scour that undermines steps [*Lenzi*, 2001; *Curran*, 2007; *Molnar et al.*, 2010], but can also rearrange particles in a way that initiates new steps; subsequent flows may continue to adjust step architecture and morphology. In the Rio Cordon, boulders found in pools, which limit pool depth and contribute to the maintenance of high velocities through pools, may have once been step formers that were undermined from downstream and collapsed into downstream pools [*Lenzi*, 2001]. The net effect of the interactions between hydraulics and morphology discussed above may be channel evolution toward some new morphologic state, in the case where positive feedbacks outweigh negative ones, or, where negative feedbacks predominate, maintenance of stable channel form.

[42] The feedbacks highlighted above also have implications for efforts to model flow resistance in step-pool channels (e.g., the work of *Comiti et al.* [2007], which is based on data from the Rio Cordon). For example, relationships between step geometry and flow resistance [e.g., *Canovaro and Solari*, 2007] and the partitioning of total resistance among spill and other components [*David et al.*, 2011] are likely influenced by details of step architecture such as leakiness or planform orientation and associated effects on velocity and turbulence variations. The effect of step leakiness on flow resistance is analogous to how drag and flow resistance produced by in-stream wood can vary depending on the porosity of wood jams [*Manners et al.*, 2007], suggesting similarities between the challenges of modeling flow resistance associated with in-stream wood and step-pool units.

4.2. Comparison to East St. Louis Creek, Colorado

[43] To further evaluate and contextualize our Rio Cordon data, here we compare the Rio Cordon to East St. Louis (ESL) Creek in the Colorado Rocky Mountains, USA. Previously we reported the results of FlowTracker ADV data collection in East St. Louis Creek at thalweg positions along step-pool sequences at five different discharges [*Wilcox and Wohl*, 2007]. East St. Louis Creek and the Rio Cordon have similar gradients, drainage areas, and subalpine settings, but differ in terms of climate, lithology, and wood loading (Table 4). The Rio Cordon has higher annual precipitation, flashier flows, and higher sediment supply. Although the Cordon has coarser bed material, the granitic lithology of ESL results in rounded boulders that are stable underfoot, in contrast to the more elongate and flat grains in the Cordon. In-stream wood is nearly absent in the Cordon study reach as a result of anthropogenic and natural factors; approximately 7% of the area upstream of our study reach is forested. In contrast, East St. Louis Creek has relatively abundant in-stream wood, 210 m^3 of wood/ha of channel [*Wohl and Jaeger*, 2009], with a contributing area that is largely forested and undisturbed by anthropogenic land uses.

[44] Many of the general characteristics of flow over step-pool sequences noted at ESL also describe the Rio Cordon. Both streams have a marked three-dimensional flow structure, albeit with downstream velocities as the largest components, and show significant variations in turbulence intensities and downstream (U) velocities with morphologic position (e.g., step versus pool) [*Wilcox and Wohl*, 2007]. Notable differences are evident, however, based on comparison of the Cordon data to data from ESL collected during analogous high-flow conditions (45–80% of $Q_{bf;}$ similar to during our Cordon measurements). Dimensionless downstream velocities (U^+) in ESL averaged 1.4 ± 1.1 in steps, 0.31 ± 0.45 in pools, and 1.1 ± 0.88 in treads. The step and pool averages are substantially lower than in the Cordon, although tread averages are similar (Figure 12, top). In addition, dimensionless turbulence intensities (RMS_u^+) are higher in ESL pools than in Cordon pools (Figure 12, bottom). These results are consistent with *Comiti et al.*'s [2007] finding that reach-scale flow velocities in the Rio Cordon, as measured using salt dilution measurements, appear to be consistently higher than in other step-pool streams of similar gradient, illustrating how hydraulics at the step-pool scale (i.e., leaky steps and fast pools in the Cordon) scale up to the reach scale.

[45] The distinct step-pool hydraulics in the two channels can be attributed to differences in step architecture and resulting jet characteristics. Whereas all steps in the Rio Cordon are formed by boulders and often have the type of gaps or other irregularities described above, steps in ESL are typically composed of a combination of clasts and wood. The wood steps in ESL produce channel-spanning obstructions, with ponding of flow upstream, critical flow across the entire

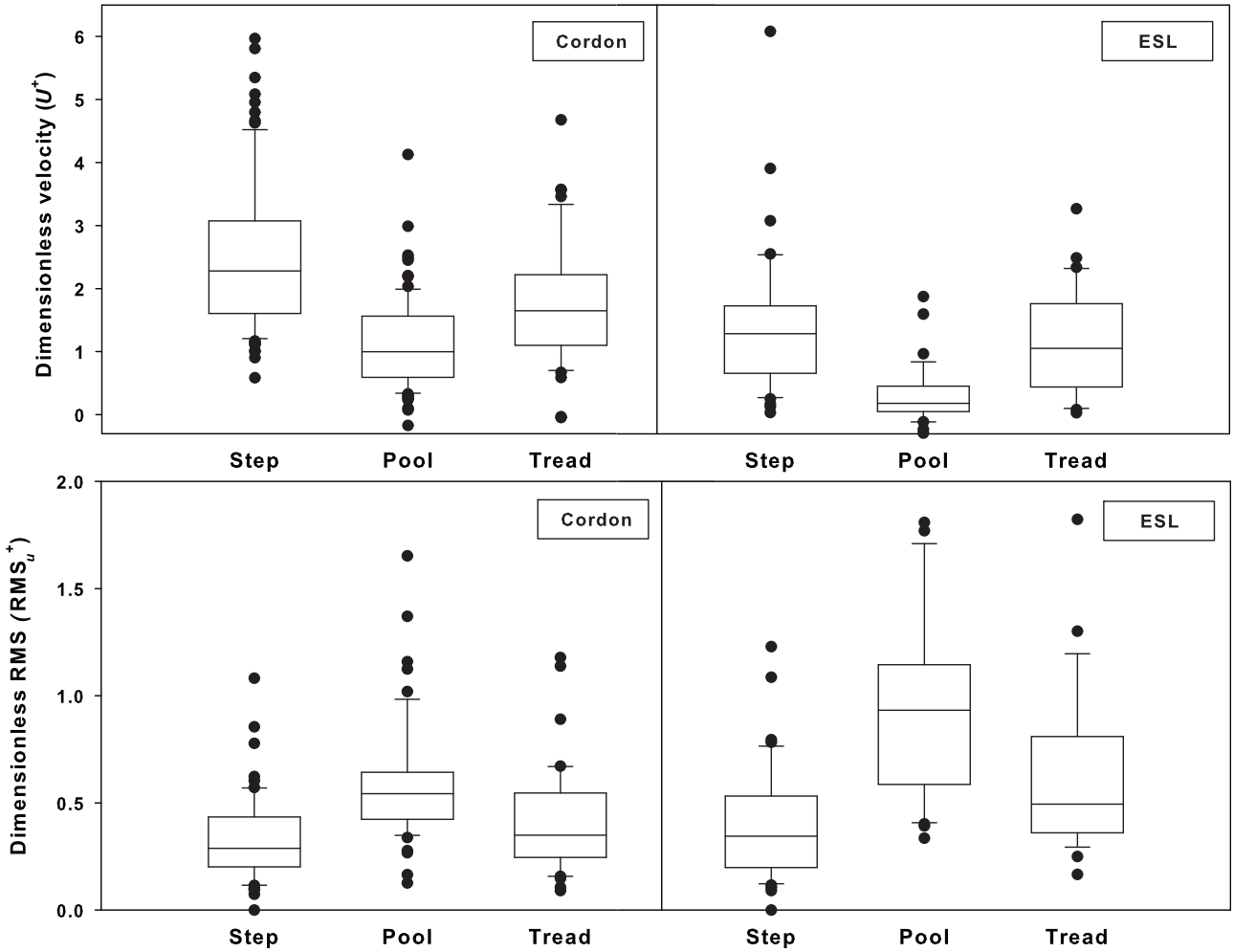

Figure 12. Comparison of (top) dimensionless downstream velocity (U^+) and (bottom) dimensionless turbulence intensity (RMS_u^+) between Rio Cordon and East St. Louis Creek by bed form type (step, pool, and tread).

crest, and a more vertical overfall downstream, resulting in greater spill resistance and slower, more turbulent pools. The presence of wood in the ESL steps does not result in greater step height, however (mean H_s in ESL was 0.54 ± 0.24 m, compared to 0.81 ± 0.31 m in the Cordon; Table 2), contrary to our expectations (based on the work of *MacFarlane and Wohl* [2003]). The greater step height in the Cordon is likely a result of larger grain sizes (Table 4); grain size is often cited as a primary control on step height [*Grant et al.*, 1990; *Chin*, 1999].

[46] Our longer-term observations of these systems suggest that East St. Louis Creek is very stable compared to the Rio Cordon in terms of the frequency of step-destabilizing floods and channel reorganization. Several events that at least partially mobilized step-forming clasts have been observed in the Rio Cordon in the last two decades [*Mao et al.*, 2010], whereas steps have been largely stable in ESL during nearly two decades of observations. Also, in the Rio Cordon the surface D_{50} of the bed is mobilized at approximately bankfull flows [*Lenzi et al.*, 2006b], which contrasts to observations in more stable stepped channels [*Bunte et al.*, 2010]. These observations highlight the combined effects of lithology, sediment supply, wood availability, and precipitation volumes and patterns on step architecture, mobility and energy dissipation. Our observations are consistent with analysis of sediment mobility in step-pool channels, including ESL, over a broader range of hydroclimatic conditions [*Wohl and Jaeger*, 2009; *Mao et al.*, 2010], and with our observations of step-pool channels along the west coast of New Zealand's South Island, where a combination of high precipitation, high sediment supply, and schist lithology that produces flattened, platy boulders result in dynamic, mobile channels despite large bed material sizes (D_{84} ~ 1 m) [*Wohl and Wilcox*, 2005]. These observations are also consistent with findings from gravel bed channels suggesting that higher sediment supply, especially of size fractions smaller than the dominant bed material size, increases the mobility of bed material [*Wilcock*, 1998; *Venditti et al.*, 2010].

[47] Step mobility and stability can viewed in the context of the above discussion of feedbacks. Step-pool channels that maintain stable morphology for longer periods can be expected to exhibit negative feedbacks between hydraulics and morphology that maintain some existing channel form. In contrast, more dynamic step-pool streams, with more frequent floods and greater sediment supply, may have positive feedbacks between hydraulics and morphology driving evolution of the channel toward a new morphologic state. Alternatively, more dynamic step-pool channels may

largely be governed by nonfluvial processes, including landslides, debris flows and woody debris input, that trump feedbacks between hydraulics and morphology as a control on channel form.

[48] Step architecture and hydraulics in the Cordon and ESL can be evaluated with respect to a recent theory for step formation, the jammed state hypothesis [*Church and Zimmermann*, 2007]. This hypothesis suggests that boulder steps represent a "jammed state" in which grains can organize into channel-spanning force chains under certain combinations of channel width (w) and grain size, where the jamming ratio is $w/D_{84(\text{step})}$ and lower ratios correspond to greater step stability [*Church and Zimmermann*, 2007]. Step formation is thus governed by ratios between channel width and boulder diameter; applied shear stress and stress needed to mobilize the bed; and bed material supply and discharge [*Zimmermann et al.*, 2010]. The jamming ratios in the Cordon and ESL are approximately 12 and 15, respectively (see Table 4 for w and D_{84}), suggesting that Cordon steps would be more stable according to the jammed state hypothesis. The observations described above suggest that wood load and particle shape can influence step stability in a manner that is not predicted by the jamming ratio. As noted above, many of the steps in the Cordon have gaps and therefore are not organized into channel-spanning force chains. Nonetheless, another recent field study, where elevated sediment transport rates were documented following step destruction by an exceptional flood in the Erlenbach, Switzerland, appears to support the jammed state hypothesis [*Turowski et al.*, 2009].

[49] Comparison of the Cordon and ESL results suggests that the jammed state hypothesis needs to be modified to account for the stabilizing effect of abundant in-stream wood pieces that are long relative to channel width and that facilitate the formation of ponded steps rather than the leaky steps more characteristic of step-pool sequences that lack in-stream wood. One of the implications of the distinction between ponded and leaky steps is that the removal of in-stream wood may result in persistent changes in step-pool morphology that effectively reduce energy dissipation and channel stability.

5. Conclusions

[50] Step-pool sequences provide an important energy dissipation mechanism in steep channels. As flow tumbles over steps and into pools, resulting in elevation loss and velocity reductions, turbulence is generated and energy is converted to heat, reflecting basic conservation of energy principles. Although velocity differences between steps and pools are much less important than elevation loss as contributors to energy dissipation, understanding of velocity structure is important with respect to aquatic habitat, near bed stresses, and flow resistance.

[51] Our measurements illuminate these characteristics with data on spatial patterns of hydraulics, step morphology, and associated energy dissipation. Relations between hydraulics and morphology for 15 step-pool sequences in the Rio Cordon, Italy, show several patterns. Porous, irregular steps and shallow, poorly developed pools with high velocities are often coupled, a condition that may be maintained by positive feedbacks that hinder the development of "jammed" steps and maintain high-velocity flow through successive step-pool sequences. Overall, approximately two thirds of energy in these reaches is dissipated by flow dropping over steps into pools. Additional energy dissipation is achieved where elevation is lost in subreaches that are not organized into steps and pools. Compared to a study site in the Colorado Rockies, the Italy study site shows many similar patterns of three-dimensional hydraulics but has notably higher pool velocities, likely as a result of differences in step architecture and in-stream wood loading.

[52] Hydraulics in steep channels defy many of the assumptions that simplify calculations of, for example, energy and momentum. Flow is nonuniform, vertical velocity profiles are nonlogarithmic [*Jarrett*, 1984; *Byrd et al.*, 2000], fluid density deviates from that of water as a result of aeration [*Vallé and Pasternack*, 2006], pressure distributions are not hydrostatic, slopes can be steep enough that the cosine of the angle of bed inclination deviates from one, and kinetic energy coefficients deviate from one [*Henderson*, 1966]. The type of data presented here provides one means toward elucidating details of hydraulics in steep channels and illustrating their distinctiveness from lower-gradient systems. Continued development of field, experimental, and computational efforts are needed, however, to develop more predictive frameworks of flow, sediment transport, and morphology of steep channels.

[53] **Acknowledgments.** Field data collection was funded by a National Science Foundation International Program grant (INT-0216951) to E.E.W. Portions of this research were performed while A.C.W. held a National Research Council postdoctoral research associateship award at the U.S. Geological Survey Geomorphology and Sediment Transport Laboratory. Funding for F.C. and L.M.'s involvement was provided by the "Epic Force" Project EC contract INCO-CT-2004-510735. We thank Andrea Andreoli for surveying assistance and Mario Lenzi for hosting A.C.W. and E.E.W.'s visit to the Rio Cordon. We also thank two anonymous reviewers for insightful comments.

References

Aberle, J., and G. M. Smart (2003), The influence of roughness structure on flow resistance on steep slopes, *J. Hydraul. Res.*, *41*(3), 259–269, doi:10.1080/00221680309499971.

Abrahams, A. D., G. Li, and J. F. Atkinson (1995), Step-pool streams: Adjustment to maximum flow resistance, *Water Resour. Res.*, *31*(10), 2593–2602, doi:10.1029/95WR01957.

Benda, L., M. A. Hassan, M. Church, and C. L. May (2005), Geomorphology of steepland headwaters: The transition from hillslopes to channels, *J. Am. Water Resour. Assoc.*, *41*(4), 835–851.

Buffin-Bélanger, T., and A. G. Roy (2005), 1 min in the life of a river: Selecting the optimal record length for the measurement of velocity in fluvial boundary layers, *Geomorphology*, *68*(1–2), 77–94, doi:10.1016/j.geomorph.2004.09.032.

Bunte, K., S. R. Abt, K. W. Swingle, and J. P. Potyondy (2010), Bankfull mobile particle size and its predictions from a Shields-type approach, paper presented at 2nd Joint Federal Interagency Conference, Las Vegas, Nev.

Byrd, T. C., D. J. Furbish, and J. Warburton (2000), Estimating depth-averaged velocities in rough channels, *Earth Surf. Processes Landforms*, *25*(2), 167–173, doi:10.1002/(SICI)1096-9837(200002)25:2<167::AID-ESP66>3.0.CO;2-G.

Canovaro, F., and L. Solari (2007), Dissipative analogies between a schematic macro-roughness arrangement and step-pool morphology, *Earth Surf. Processes Landforms*, *32*(11), 1628–1640, doi:10.1002/esp.1590.

Chanson, H. (1994), *Hydraulic Design of Stepped Cascades, Channels, Weirs and Spillways*, 261 pp., Pergamon, Oxford, U. K.

Chanson, H. (1996), Comment on "Step-pool streams: Adjustment to maximum flow resistance" by Athol D. Abrahams, Gang Li, and Joseph F. Atkinson, *Water Resour. Res.*, *32*(11), 3401–3402, doi:10.1029/96WR02314.

Chartrand, S. M., and P. J. Whiting (2000), Alluvial architecture in headwater streams with special emphasis on step-pool topography, *Earth*

Surf. Processes Landforms, *25*(6), 583–600, doi:10.1002/1096-9837(200006)25:6<583::AID-ESP92>3.0.CO;2-3.

Chin, A. (1999), The morphologic structure of step-pools in mountain streams, *Geomorphology*, *27*(3–4), 191–204, doi:10.1016/S0169-555X(98)00083-X.

Chin, A. (2002), The periodic nature of step-pool mountain streams, *Am. J. Sci.*, *302*(2), 144–167, doi:10.2475/ajs.302.2.144.

Chin, A., and J. D. Phillips (2007), The self-organization of step-pools in mountain streams, *Geomorphology*, *83*(3–4), 346–358, doi:10.1016/j.geomorph.2006.02.021.

Chin, A., and E. Wohl (2005), Toward a theory for step pools in stream channels, *Prog. Phys. Geogr.*, *29*(3), 275–296, doi:10.1191/0309133305pp449ra.

Chin, A., et al. (2009), Linking theory and practice for restoration of step-pool streams, *Environ. Manage. N. Y.*, *43*(4), 645–661, doi:10.1007/s00267-008-9171-x.

Church, M., and A. Zimmermann (2007), Form and stability of step-pool channels: Research progress, *Water Resour. Res.*, *43*, W03415, doi:10.1029/2006WR005037.

Clifford, N. J., and J. R. French (1993), Monitoring and modelling turbulent flow: Historical and contemporary perspectives, in *Turbulence: Perspectives on Flow and Sediment Transport*, edited by N. J. Clifford et al., pp. 1–34, John Wiley, Chichester, U. K.

Comiti, F., and M. A. Lenzi (2006), Dimensions of standing waves at steps in mountain rivers, *Water Resour. Res.*, *42*, W03411, doi:10.1029/2004WR003898.

Comiti, F., and L. Mao (2011), Recent advances on the dynamics of steep channels, in *Gravel Bed Rivers 7*, edited by M. Church, P. Biron, and A. Roy, John Wiley, Chichester, U. K.

Comiti, F., A. Andreoli, and M. A. Lenzi (2005), Morphological effects of local scouring in step-pool streams, *Earth Surf. Processes Landforms*, *30*(12), 1567–1581, doi:10.1002/esp.1217.

Comiti, F., A. Andreoli, M. A. Lenzi, and L. Mao (2006), Spatial density and characteristics of woody debris in five mountain rivers of the Dolomites (Italian Alps), *Geomorphology*, *78*(1–2), 44–63, doi:10.1016/j.geomorph.2006.01.021.

Comiti, F., L. Mao, A. Wilcox, E. E. Wohl, and M. A. Lenzi (2007), Field-derived relationships for flow velocity and resistance in high-gradient streams, *J. Hydrol.*, *340*(1–2), 48–62, doi:10.1016/j.jhydrol.2007.03.021.

Comiti, F., D. Cadol, and E. Wohl (2009a), Flow regimes, bed morphology, and flow resistance in self-formed step-pool channels, *Water Resour. Res.*, *45*, W04424, doi:10.1029/2008WR007259.

Comiti, F., L. Mao, M. A. Lenzi, and M. Siligardi (2009b), Artificial steps to stabilize mountain rivers: A post-project ecological assessment, *River Res. Appl.*, *25*(5), 639–659, doi:10.1002/rra.1234.

Curran, J. C. (2007), Step-pool formation models and associated step spacing, *Earth Surf. Processes Landforms*, *32*(11), 1611–1627, doi:10.1002/esp.1589.

Curran, J. H., and E. E. Wohl (2003), Large woody debris and flow resistance in step-pool channels, Cascade Range, Washington, *Geomorphology*, *51*(1–3), 141–157, doi:10.1016/S0169-555X(02)00333-1.

D'Agostino, V., and M. A. Lenzi (1999), Bedload transport in the instrumented catchment of the Rio Cordon: Part II—Analysis of the bedload rate, *Catena*, *36*(3), 191–204, doi:10.1016/S0341-8162(99)00017-X.

David, G. C. L., E. Wohl, S. E. Yochum, and B. P. Bledsoe (2010), Controls on spatial variations in flow resistance along steep mountain streams, *Water Resour. Res.*, *46*, W03513, doi:10.1029/2009WR008134.

David, G. C. L., E. Wohl, S. E. Yochum, and B. P. Bledsoe (2011), Comparative analysis of bed resistance partitioning in high gradient streams, *Water Resour. Res.*, doi:10.1029/2010WR009540, in press.

Dingman, S. L. (2009), *Fluvial Hydraulics*, 559 pp., Oxford Univ. Press, New York.

Ferguson, R. (2007), Flow resistance equations for gravel- and boulder-bed streams, *Water Resour. Res.*, *43*, W05427, doi:10.1029/2006WR005422.

Fontana, G. D., and L. Marchi (2003), Slope-area relationships and sediment dynamics in two alpine streams, *Hydrol. Processes*, *17*(1), 73–87, doi:10.1002/hyp.1115.

Freeman, M. C., C. M. Pringle, and C. R. Jackson (2007), Hydrologic connectivity and the contribution of stream headwaters to ecological integrity at regional scales, *J. Am. Water Resour. Assoc.*, *43*(1), 5–14, doi:10.1111/j.1752-1688.2007.00002.x.

Gintz, D., M. A. Hassan, and K. H. Schmidt (1996), Frequency and magnitude of bedload transport in a mountain river, *Earth Surf. Processes Landforms*, *21*(5), 433–445, doi:10.1002/(SICI)1096-9837(199605)21:5<433::AID-ESP580>3.0.CO;2-P.

Goring, D. G., and V. I. Nikora (2002), Despiking acoustic Doppler velocimeter data, *J. Hydraul. Eng.*, *128*(1), 117–126, doi:10.1061/(ASCE)0733-9429(2002)128:1(117).

Grant, G. E., F. J. Swanson, and M. G. Wolman (1990), Pattern and origin of stepped-bed morphology in high-gradient streams, western Cascades, Oregon, *Geol. Soc. Am. Bull.*, *102*(3), 340–352, doi:10.1130/0016-7606(1990)102<0340:PAOOSB>2.3.CO;2.

Hayward, J. A. (1980), *Hydrology and Stream Sediments in a Mountain Catchment*, *Tussock Grasslands Mt. Lands Inst. Spec. Publ.*, vol. 17, 236 pp., Lincoln Coll., Canterbury, New Zealand.

Henderson, F. M. (1966), *Open Channel Flow*, 522 pp., Macmillan, New York.

Jarrett, R. D. (1984), Hydraulics of high-gradient streams, *J. Hydraul. Eng.*, *110*(11), 1519–1539, doi:10.1061/(ASCE)0733-9429(1984)110:11(1519).

Keller, E. A., and F. J. Swanson (1979), Effects of large organic material on channel form and fluvial processes, *Earth Surf. Processes Landforms*, *4*(4), 361–380.

Lamarre, H., and A. G. Roy (2005), Reach scale variability of turbulent flow characteristics in a gravel-bed river, *Geomorphology*, *68*(1–2), 95–113, doi:10.1016/j.geomorph.2004.09.033.

Lee, A. J., and R. I. Ferguson (2002), Velocity and flow resistance in step-pool streams, *Geomorphology*, *46*(1–2), 59–71, doi:10.1016/S0169-555X(02)00054-5.

Legleiter, C. J., T. L. Phelps, and E. E. Wohl (2007), Geostatistical analysis of the effects of stage and roughness on reach-scale spatial patterns of velocity and turbulence intensity, *Geomorphology*, *83*(3–4), 322–345, doi:10.1016/j.geomorph.2006.02.022.

Lenzi, M. A. (2001), Step-pool evolution in the Rio Cordon, northeastern Italy, *Earth Surf. Processes Landforms*, *26*(9), 991–1008, doi:10.1002/esp.239.

Lenzi, M. A. (2002), Stream bed stabilization using boulder check dams that mimic step-pool morphology features in northern Italy, *Geomorphology*, *45*(3–4), 243–260, doi:10.1016/S0169-555X(01)00157-X.

Lenzi, M. A. (2004), Displacement and transport of marked pebbles, cobbles and boulders during floods in a steep mountain stream, *Hydrol. Processes*, *18*(10), 1899–1914, doi:10.1002/hyp.1456.

Lenzi, M. A., V. D'Agostino, and P. Billi (1999), Bedload transport in the instrumented catchment of the Rio Cordon: Part I—Analysis of bedload records, conditions and threshold of bedload entrainment, *Catena*, *36*(3), 171–190, doi:10.1016/S0341-8162(99)00016-8.

Lenzi, M. A., L. Mao, and F. Comiti (2003), Interannual variation of suspended sediment load and sediment yield in an alpine catchment, *Hydrol. Sci. J.*, *48*(6), 899–915, doi:10.1623/hysj.48.6.899.51425.

Lenzi, M. A., L. Mao, and F. Comiti (2004), Magnitude-frequency analysis of bed load data in an Alpine boulder bed stream, *Water Resour. Res.*, *40*, W07201, doi:10.1029/2003WR002961.

Lenzi, M. A., L. Mao, and F. Comiti (2006a), When does bedload transport begin in steep boulder-bed streams?, *Hydrol. Processes*, *20*(16), 3517–3533, doi:10.1002/hyp.6168.

Lenzi, M. A., L. Mao, and F. Comiti (2006b), Effective discharge for sediment transport in a mountain river: Computational approaches and geomorphic effectiveness, *J. Hydrol.*, *326*(1–4), 257–276, doi:10.1016/j.jhydrol.2005.10.031.

Leutheusser, H. J., and W. M. Birk (1991), Drownproofing of low overflow structures, *J. Hydraul. Eng.*, *117*(2), 205–213, doi:10.1061/(ASCE)0733-9429(1991)117:2(205).

MacFarlane, W. A., and E. Wohl (2003), Influence of step composition on step geometry and flow resistance in step-pool streams of the Washington Cascades, *Water Resour. Res.*, *39*(2), 1037, doi:10.1029/2001WR001238.

MacVicar, B. J., and A. G. Roy (2007), Hydrodynamics of a forced riffle pool in a gravel bed river: 1. Mean velocity and turbulence intensity, *Water Resour. Res.*, *43*, W12401, doi:10.1029/2006WR005272.

MacVicar, B. J., E. Beaulieu, V. Champagne, and A. G. Roy (2007), Measuring water velocity in highly turbulent flows: Field tests of an electromagnetic current meter (ECM) and an acoustic Doppler velocimeter (ADV), *Earth Surf. Processes Landforms*, *32*(9), 1412–1432, doi:10.1002/esp.1497.

Manners, R. B., M. W. Doyle, and M. J. Small (2007), Structure and hydraulics of natural woody debris jams, *Water Resour. Res.*, *43*, W06432, doi:10.1029/2006WR004910.

Mao, L., and M. A. Lenzi (2007), Sediment mobility and bedload transport conditions in an alpine stream, *Hydrol. Processes*, *21*(14), 1882–1891, doi:10.1002/hyp.6372.

Mao, L., M. Cavalli, F. Comiti, L. Marchi, M. A. Lenzi, and M. Arattano (2009), Sediment transfer processes in two Alpine catchments of contrasting morphological settings, *J. Hydrol.*, *364*(1–2), 88–98, doi:10.1016/j.jhydrol.2008.10.021.

Mao, L., F. Comiti, and M. A. Lenzi (2010), Bedload dynamics in steep mountain rivers: Insights from the Rio Cordon experimental station (Italian Alps), in *Bedload-Surrogate Monitoring Technologies*, edited by J. R. Gray, J. B. Laronne, and J. D. G. Marr, *U.S. Geol. Surv. Sci. Invest. Rep.*, *2010-5091*, 253–265.

Marion, A., M. A. Lenzi, and F. Comiti (2004), Effect of sill spacing and sediment size grading on scouring at grade-control structures, *Earth Surf. Processes Landforms*, *29*(8), 983–993, doi:10.1002/esp.1081.

Marston, R. A. (1982), The geomorphic significance of log steps in forest streams, *Ann. Assoc. Am. Geogr.*, *72*, 99–108, doi:10.1111/j.1467-8306.1982.tb01386.x.

Middleton, G. V., and P. R. Wilcock (1994), *Mechanics in the Earth and Environmental Sciences*, Cambridge Univ. Press, Cambridge, U. K.

Milzow, C., P. Molnar, B. W. McArdell, and P. Burlando (2006), Spatial organization in the step-pool structure of a steep mountain stream (Vogelbach, Switzerland), *Water Resour. Res.*, *42*, W04418, doi:10.1029/2004WR003870.

Molnar, P., A. L. Densmore, B. W. McArdell, J. M. Turowski, and P. Burlando (2010), Analysis of changes in the step-pool morphology and channel profile of a steep mountain stream following a large flood, *Geomorphology*, *124*(1–2), 85–94, doi:10.1016/j.geomorph.2010.08.014.

Montgomery, D. R., and J. M. Buffington (1997), Channel-reach morphology in mountain drainage basins, *Geol. Soc. Am. Bull.*, *109*(5), 596–611, doi:10.1130/0016-7606(1997)109<0596:CRMIMD>2.3.CO;2.

Moore, W. L. (1943), Energy loss at the base of a free overfall, *Trans. Am. Soc. Civ. Eng.*, *108*, 1343–1360.

Nezu, I., and H. Nakagawa (1993), *Turbulence in Open-Channel Flows*, 281 pp., A. A. Balkema, Rotterdam, Netherlands.

Nickolotsky, A., and R. T. Pavlowsky (2007), Morphology of step-pools in a wilderness headwater stream: The importance of standardizing geomorphic measurements, *Geomorphology*, *83*(3–4), 294–306, doi:10.1016/j.geomorph.2006.02.025.

Nikora, V. I., and D. G. Goring (1998), ADV measurements of turbulence: Can we improve their interpretation?, *J. Hydraul. Eng.*, *124*(6), 630–634, doi:10.1061/(ASCE)0733-9429(1998)124:6(630).

Pasternack, G. B., C. R. Ellis, K. A. Leier, B. L. Vallé, and J. D. Marr (2006), Convergent hydraulics at horseshoe steps in bedrock rivers, *Geomorphology*, *82*(1–2), 126–145, doi:10.1016/j.geomorph.2005.08.022.

Rajaratnam, N., and M. R. Chamani (1995), Energy loss at drops, *J. Hydraul. Res.*, *33*, 373–384, doi:10.1080/00221689509498578.

Rehmel, M. (2007), Application of acoustic Doppler velocimeters for streamflow measurements, *J. Hydraul. Eng.*, *133*(12), 1433–1438, doi:10.1061/(ASCE)0733-9429(2007)133:12(1433).

Rickenmann, D. (1991), Hyperconcentrated flow and sediment transport at steep slopes, *J. Hydraul. Eng.*, *117*(11), 1419–1439, doi:10.1061/(ASCE)0733-9429(1991)117:11(1419).

Roberson, J. A., and C. T. Crowe (1997), *Engineering Fluid Mechanics*, 6th ed., John Wiley, New York.

Rodriguez, A., A. Sánchez-Arcilla, J. M. Redondo, and C. Mösso (1999), Macroturbulence measurements with electromagnetic and ultrasonic sensors: A comparison under high-turbulent flows, *Exp. Fluids*, *27*(1), 31–42, doi:10.1007/s003480050326.

SonTek (2001), FlowTracker handheld ADV technical documentation, San Diego, Calif.

Trevisani, S., M. Cavalli, and L. Marchi (2010), Reading the bed morphology of a mountain stream: A geomorphometric study on high-resolution topographic data, *Hydrol. Earth Syst. Sci.*, *14*, 393–405, doi:10.5194/hess-14-393-2010.

Turowski, J. M., E. M. Yager, A. Badoux, D. Rickenmann, and P. Molnar (2009), The impact of exceptional events on erosion, bedload transport and channel stability in a step-pool channel, *Earth Surf. Processes Landforms*, *34*(12), 1661–1673, doi:10.1002/esp.1855.

Bureau of Reclamation (1948), Studies of crests for overfall dams, in *Boulder Canyon Project, Hydraulic Investigations*, part VI, bull. 3, Dep. of the Inter., Denver, Colo.

Vallé, B. L., and G. B. Pasternack (2002), TDR measurements of hydraulic jump aeration in the South Fork of the American River, California, *Geomorphology*, *42*(1–2), 153–165, doi:10.1016/S0169-555X(01)00083-6.

Vallé, B. L., and G. B. Pasternack (2006), Air concentrations of submerged and unsubmerged hydraulic jumps in a bedrock step-pool channel, *J. Geophys. Res.*, *111*, F03016, doi:10.1029/2004JF000140.

Venditti, J. G., W. E. Dietrich, P. A. Nelson, M. A. Wydzga, J. Fadde, and L. Sklar (2010), Mobilization of coarse surface layers in gravel-bedded rivers by finer gravel bed load, *Water Resour. Res.*, *46*, W07506, doi:10.1029/2009WR008329.

Weichert, R. B., G. R. Bezzola, and H.-E. Minor (2008), Bed morphology and generation of step-pool channels, *Earth Surf. Processes Landforms*, *33*(11), 1678–1692, doi:10.1002/esp.1639.

Wilcock, P. R. (1998), Two-fraction model of initial sediment motion in gravel-bed rivers, *Science*, *280*, 410–412, doi:10.1126/science.280.5362.410.

Wilcox, A. C., and E. E. Wohl (2006), Flow resistance dynamics in step-pool channels: 1. Large woody debris and controls on total resistance, *Water Resour. Res.*, *42*, W05418, doi:10.1029/2005WR004277.

Wilcox, A. C., and E. E. Wohl (2007), Field measurements of three-dimensional hydraulics in a step-pool channel, *Geomorphology*, *83*(3–4), 215–231, doi:10.1016/j.geomorph.2006.02.017.

Wilcox, A. C., J. M. Nelson, and E. E. Wohl (2006), Flow resistance dynamics in step-pool channels: 2. Partitioning between grain, spill, and woody debris resistance, *Water Resour. Res.*, *42*, W05419, doi:10.1029/2005WR004278.

Wohl, E. E. (2000), *Mountain Rivers*, *Water Resour. Monogr.*, vol. 14, 320 pp., AGU, Washington, D. C.

Wohl, E. E., and T. Grodek (1994), Channel bed-steps along Nahal-Yael, Negev Desert, Israel, *Geomorphology*, *9*(2), 117–126, doi:10.101b 6/0169-555X(94)90070-1.

Wohl, E., and K. L. Jaeger (2009), Geomorphic implications of hydroclimatic differences among step-pool channels, *J. Hydrol.*, *374*(1–2), 148–161, doi:10.1016/j.jhydrol.2009.06.008.

Wohl, E. E., and D. M. Thompson (2000), Velocity characteristics along a small step-pool channel, *Earth Surf. Processes Landforms*, *25*(4), 353–367, doi:10.1002/(SICI)1096-9837(200004)25:4<353::AID-ESP59>3.0.CO;2-5.

Wohl, E. E., and A. Wilcox (2005), Channel geometry of mountain streams in New Zealand, *J. Hydrol.*, *300*(1–4), 252–266, doi:10.1016/j.jhydrol.2004.06.006.

Wu, S., and N. Rajaratnam (1996), Transition from hydraulic jump to open channel flow, *J. Hydraul. Eng.*, *122*(9), 526–528, doi:10.1061/(ASCE)0733-9429(1996)122:9(526).

Wu, S., and N. Rajaratnam (1998), Impinging jet and surface flow regimes at drop, *J. Hydraul. Res.*, *36*(1), 69–74, doi:10.1080/00221689809498378.

Wyrick, J. R., and G. B. Pasternack (2008), Modeling energy dissipation and hydraulic jump regime responses to channel nonuniformity at river steps, *J. Geophys. Res.*, *113*, F03003, doi:10.1029/2007JF000873.

Zimmermann, A. (2010), Flow resistance in steep streams: An experimental study, *Water Resour. Res.*, *46*, W09536, doi:10.1029/2009WR007913.

Zimmermann, A., and M. Church (2001), Channel morphology, gradient profiles and bed stresses during flood in a step-pool channel, *Geomorphology*, *40*(3–4), 311–327, doi:10.1016/S0169-555X(01)00057-5.

Zimmermann, A. E., M. Church, and M. A. Hassan (2008), Identification of steps and pools from stream longitudinal profile data, *Geomorphology*, *102*(3–4), 395–406, doi:10.1016/j.geomorph.2008.04.009.

Zimmermann, A., M. Church, and M. A. Hassan (2010), Step-pool stability: Testing the jammed state hypothesis, *J. Geophys. Res.*, *115*, F02008, doi:10.1029/2009JF001365.

F. Comiti, Faculty of Science and Technology, Free University of Bozen-Bolzano, piazza Università 5, I-39100 Bolzano, Italy. (francesco.comiti@unibz.it)

L. Mao, Department of Land and Agro-Forest Environments, University of Padova, Agripolis viale Università 16, I-35020 Legnaro, Italy. (luca.mao@unipd.it)

A. C. Wilcox, Department of Geosciences, University of Montana, 32 Campus Dr. 1296, Missoula, MT 59812, USA. (andrew.wilcox@umontana.edu)

E. E. Wohl, Department of Geosciences, Colorado State University, Fort Collins, CO 80523, USA. (ellenw@warnercnr.colostate.edu)